Journal of Medicinal Chemistry

Article

Depsipeptides featuring a neutral P1 are potent inhibitors of kallikrein-related peptidase 6 with on-target cellular activity

Elena De Vita, Peter Schüler, Scott Lovell, Jasmin Lohbeck, Sven Kullmann, Eitan Rabinovich, Amiram Sananes, Bernd Heßling, Veronique Hamon, Niv Papo, Jochen Heß, Edward W. Tate, Nikolas Gunkel, and Aubry K. Miller

J. Med. Chem., **Just Accepted Manuscript** • DOI: 10.1021/acs.jmedchem.8b01106 • Publication Date (Web): 13 Sep 2018

ACS Publications

is published by the American Chemical Society. 1155 Sixteenth Street N.W., Washington, DC 20036

Depsipeptides featuring a neutral P1 are potent inhibitors of kallikrein-related peptidase 6 with on-target cellular activity

Elena De Vita,[a,b] *Peter Schüler,*[a] *Scott Lovell,*[c] *Jasmin Lohbeck,*[a] *Sven Kullmann,*[a] *Eitan Rabinovich,*[d] *Amiram Sananes,*[d] *Bernd Heßling,*[e,†] *Veronique Hamon,*[f] *Niv Papo,*[d] *Jochen Hess,*[g,h] *Edward W. Tate,*[c] *Nikolas Gunkel*[a,i] *and Aubry K. Miller**[a,i]

[a] Cancer Drug Development Group, German Cancer Research Center (DKFZ), Heidelberg 69120, Germany

[b] Biosciences Faculty, University of Heidelberg, Heidelberg 69120, Germany

[c] Department of Chemistry, Imperial College London, Exhibition Road, London SW7 2AZ, UK

[d] Department of Biotechnology Engineering and the National Institute of Biotechnology in the Negev, Ben-Gurion University of the Negev, Beer-Sheva 84105, Israel

[e] Center for Molecular Biology, University of Heidelberg, Heidelberg 69120, Germany

[f] European Screening Centre, Biocity Scotland, University of Dundee, Newhouse ML1 5UH, UK

[g] Department of Otorhinolaryngology, Head and Neck Surgery, Heidelberg University Hospital, Heidelberg 69120, Germany

[h] Research Group Molecular Mechanisms of Head and Neck Tumors, German Cancer Research Center (DKFZ), Heidelberg 69120, Germany

[i] German Cancer Consortium (DKTK), Heidelberg 69120, Germany

ABSTRACT

Kallikrein-related peptidase 6 (KLK6) is a secreted serine protease that belongs to the family of tissue kallikreins (KLKs). Many KLKs are investigated as potential biomarkers for cancer as well as therapeutic drug targets for a number of pathologies. KLK6, in particular, has been implicated in neurodegenerative diseases and cancer, but target validation has been hampered by a lack of selective inhibitors. This work introduces a class of depsipeptidic KLK6 inhibitors, discovered via high-throughput screening, which were found to function as substrate mimics that transiently acylate the catalytic serine of KLK6. Detailed structure–activity relationship studies, aided by in silico modeling, uncovered strict structural requirements for potency, stability, and acyl-enzyme complex half-life. An optimized scaffold, DKFZ-251, demonstrated good selectivity for KLK6 compared to other KLKs, and on-target activity in a cellular assay. Moreover, DKFZ-633, an inhibitor-derived activity-based probe, could be used to pull down active endogenous KLK6.

INTRODUCTION

The largest protease gene cluster in the human genome encodes a family of 15 secreted serine proteases commonly known as the tissue kallikreins (KLKs), which encompass human tissue kallikrein (KLK1) and 14 kallikrein-related peptidases (KLK2–15). Once considered to function

largely as redundant extracellular matrix-degrading enzymes, it is now well recognized that KLKs are critical regulators of finely tuned and complex cascade systems[1] (e.g. skin desquamation, brain function, seminal liquefaction, and immune control), with tissue-dependent expression and function.[2] Beyond their physiological roles, aberrant KLK expression and activity have been implicated in a variety of pathologies, including skin diseases, neurological disorders, and cancer.[3] In the latter case, KLKs are extensively studied as biomarkers.[4] For example, KLK3, more commonly known as prostate-specific antigen (PSA), is one of the most well-known of all cancer biomarkers.[5] In addition to their usefulness as clinical markers, KLKs are now considered to directly contribute to a variety of cancer hallmarks, such as chemo-resistance, cell growth, invasion, migration, and modulation of the tumor microenvironment.[3a] Due to a lack of high quality, selective activity-based probes (ABPs), however, few attempts to quantify the active enzyme fraction of endogenous KLK proteins have been made.[6]

Despite being one of the most abundant proteinases in the central nervous system, very little is known about kallikrein-related peptidase 6 (KLK6). Four different groups isolated KLK6 in the mid-1990s, and, not immediately recognizing that they were working with the same protein, gave it multiple names, i.e. Protease M, Zyme, Neurosin, and Myelencephalon-specific protease.[7] After the sequencing of the human genome, KLK6 was correctly classified as a member of the kallikrein family, and by then had captured attention for being highly expressed in breast and ovarian cancer.[7a] KLK6 is secreted in its zymogen pro-form and activated via proteolytic cleavage (Lys15↓Leu16). Auto-inactivation can occur via hydrolysis at Arg76↓Glu77 and this has been postulated as a negative-feedback inhibition mechanism.[8] In vitro studies have shown that this protease is able to cleave myelin basic protein, alpha-synuclein, and the beta-amyloid

precursor protein.[7b,9] Moreover, it can activate protease-activated receptors (PARs), thus triggering intracellular signaling and influencing cellular processes.[10] Aberrant expression of KLK6 has been reported in various neurodegenerative diseases such as multiple sclerosis, Alzheimer's, and Parkinson's disease.[9b, 11] Notably, two studies involving auto-immunization of a multiple sclerosis mouse model with KLK6-neutralizing antibodies showed a significantly delayed onset and reduced severity of the disease.[12] Recent reports have also suggested that KLK6 is an active driver of tumor development. Keratinocytes within the malignant melanoma microenvironment, but not primary tumor cells, produce high amounts of KLK6, which then promotes tumor migration and invasiveness via the activation of protease-activated receptor 1 (PAR1).[13] In ovarian cancer, KLK6 overexpression negatively correlates with survival and has also been postulated to play a role in tumor invasiveness.[14] In gastric cancer[15] and glioblastoma,[16] KLK6 has been shown to contribute to therapy resistance. In head and neck cancer on the other hand, KLK6 silencing was found to promote cell proliferation and an epithelial to mesenchymal transition (EMT).[17]

While the field of KLK inhibitor discovery is relatively underdeveloped, recent reviews highlight the interest and need for further work.[1a, 18] A common approach for the development of inhibitors has been to utilize natural peptidic inhibitors as starting points, exploiting combinatorial or designed mutations in order to achieve selectively toward the targeted KLK. Still, the development of sub-type selective KLK inhibitors remains challenging.[19] Better success has been achieved with the chymotryptic-like KLK7, which has unique substrate specificity in comparison to other KLKs.[20] To the best of our knowledge, four accounts of small molecule KLK6 inhibitors exist to date, including two classes of small molecules discovered by virtual screen,[21] a series of pseudopeptides (based on the activating peptide of PAR2),[22] and a recent

coumarin-derived mechanism-based inhibitor[23] (Chart 1). As most of these reports show no data for activity against related proteases, the selectivity of these compounds remains unknown at present. KLK6, like most other KLKs, has trypsin-like activity, governed by an acidic Asp189 (trypsin numbering) in the S1 pocket, which dictates the preference for a basic arginine or lysine residue in P1 of KLK6 substrates. KLK6 also contains a Ser190, a feature that has been found particularly difficult to target with neutral P1 inhibitors, with few examples in the literature.[24] Usually, inhibitors of Ser190-containing proteases require the presence of a strongly basic residue in P1 for binding, but this can lead to unfavorable pharmacological properties due to the inherent charged state of the molecules.[25] In addition, the highly conserved nature of Asp189 (and Ser190 when present) in the S1 pocket of trypsin-like serine proteases has been recognized to complicate the development of selective inhibitors.[26] Motivated by the pressing need for selective KLK6 chemical probes for use as validation tools for in depth biological studies, and aware of the existing challenges, we set out to discover potent and selective inhibitors of KLK6.

Chart 1. Known KLK6 inhibitors.

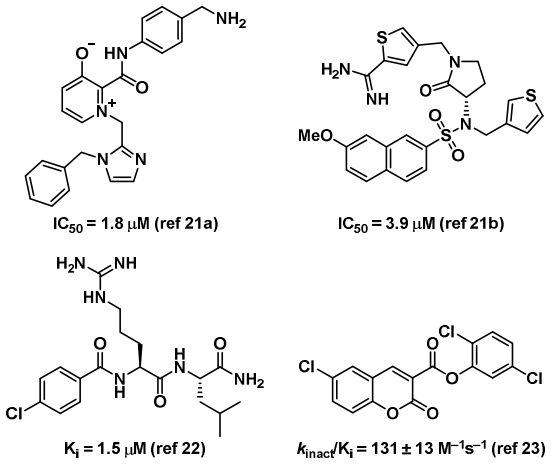

RESULTS AND DISCUSSION

High Throughput Screening Provides a Neutral Depsipeptidic Hit Scaffold

In order to discover novel KLK6 inhibitors, we chose a high-throughput screen (HTS) approach at the outset of this project. A triple mutant of KLK6 (R74G, R76Q, and N132Q), resistant to autocleavage and lacking a glycosylation site, was recombinantly expressed in insect cells, and purified as previously reported (Figure S1).[21a,27] An enzymatic assay, which monitors the activity of KLK6 by cleavage of the fluorogenic substrate *N*-Boc-Phe-Ser-Arg-7-amino-4-methylcoumarin (FSR-AMC), was optimized for HTS and validated with the known inhibitors AEBSF and gabexate. After a successful pilot screen (Figure S2), a full HTS of a library of more than 80,000 substances tested at 40 μM gave a hit rate of 0.05% when applying a threshold cut-off at 30% inhibition of substrate turnover (Figure 1A).

Dose response curves of 124 hits were determined in duplicate and 18 substances were found to have IC_{50} values between 10–100 μM. These 18 hits were grouped into similarity clusters and singletons, and 123 structurally related substances were ordered from commercial vendors. The resulting 141 compounds were then tested in dose response against KLK6, and commercially sourced trypsin, thrombin and factor Xa. These other three serine proteases were selected as a counter selectivity screen due to their close structural similarity with KLK6 and to their physiological importance. The selectivity screen revealed only one class of substances, a series of depsipeptides (e.g. **1–5**), which exhibited at least low micromolar IC_{50} values against KLK6 and some selectivity against all three other peptidases (Figure 1B). We found that while some activity against trypsin was observed with these substances, they were generally quite inactive against both factor Xa and thrombin. Encouragingly, some structurally similar substances (e.g., **1**, **2** and **5**) had very different IC_{50} values against KLK6, giving us some confidence that the hits were "true" positives. The general structure of these substances can be dissected into three main components: the depsipeptidic glycolic linker (L, Figure 1B, black), which is flanked by a

"western" aromatic group (W, Figure 1B, blue) and an "eastern" N-phenyl-4-amino-3,5-dimethylpyrazole (E, Figure 1B, red). Compound **1**, containing a western N-linked 2-methylindole stood out as having the best combination of potency against KLK6 and selectivity over trypsin (IC_{50}s of 640 nM and 70 µM, respectively). We were further intrigued by the conspicuous lack of a strongly basic group in **1**, and were cautiously optimistic about the possibility to develop a selective inhibitor for a Ser190-containing serine protease.

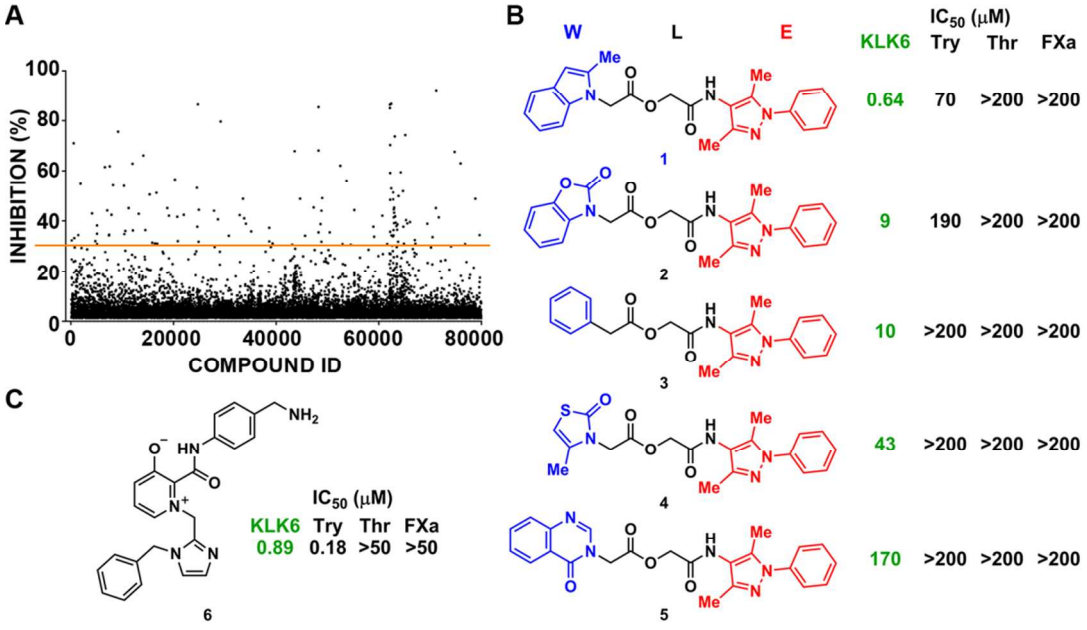

Figure 1. HTS and selectivity screen results. (A) Graphical representation of an HTS, which measured reduced turnover of FSR-AMC by KLK6. Inhibitors were tested at 40 µM. Orange line represents 30% inhibition cut-off. (B) Structures of five depsipeptides and their measured IC_{50} values against four proteases. Main structural features are defined by color code: W (blue) = "western" aromatic group; L (black) = depsipeptidic linker; E (red) = "eastern" aromatic group. (C) Structure and IC_{50} data of the previously reported inhibitor **6**. Try = trypsin; Thr = thrombin; FXa = factor Xa.

We also prepared the known zwitterionic KLK6 inhibitor **6** as a validation compound, and determined its selectivity profile (Figure 1C).[21a] The measured KLK6 IC_{50} value was in accordance with the literature (measured: 890 nM; reported: 1.8 μM) and the substance was found to potently inhibit trypsin (IC_{50} = 180 nM), while being ineffective against both thrombin and factor Xa. The fact that **6** inhibits trypsin well is perhaps not surprising considering its high homology with KLK6 and that **6** contains a basic polar benzylamine P1 group.

Depsipeptides Act as Transient Quiescent Affinity Labelers of KLK6

The depsipeptidic structure of **1**, which contains an electrophilic ester functional group, gave rise to the question whether the substance might function as a covalent inhibitor of KLK6.[28] We therefore prepared a fully peptidic analog (**7**) as well as carbamate **8** (Figure 2A).[29] These were found to be inactive against KLK6, suggesting that reaction of the ester bond is required for compound activity. Moreover, methyl ester **9** and acetate **10** were prepared so as to "isolate" the western and eastern portions, respectively (Figure 2A). Both **9** and **10** were inactive against KLK6, showing that while the central ester bond of **1** is required for activity, both the western and eastern moieties must also be in place. Nano-flow reverse-phase chromatography combined with electrospray ionization mass spectrometry (ESI-MS) of the intact protein (7 μM KLK6, Figure S3) incubated with excess **1** (200 μM) was performed, and, after 1 h, a mass shift of 171 Da was observed with no un-modified protein detected (Figure 2B). This mass shift corresponds to the carboxy part of ester **1**. Conducting this experiment with analogs of **1** bearing different W groups gave different mass shifts (Figure S4). In addition, **11** (DKFZ-251), a regioisomer of **1**, produced the same 171 Da shift (Figure 2B). Tryptic digest of the modified enzyme showed a 171 Da shift only on those peptides containing Ser195 (Figure S5), and ESI-MS of an Ser195A mutant indicated no mass shift when treating with **1** or **11** (Figure 2B).

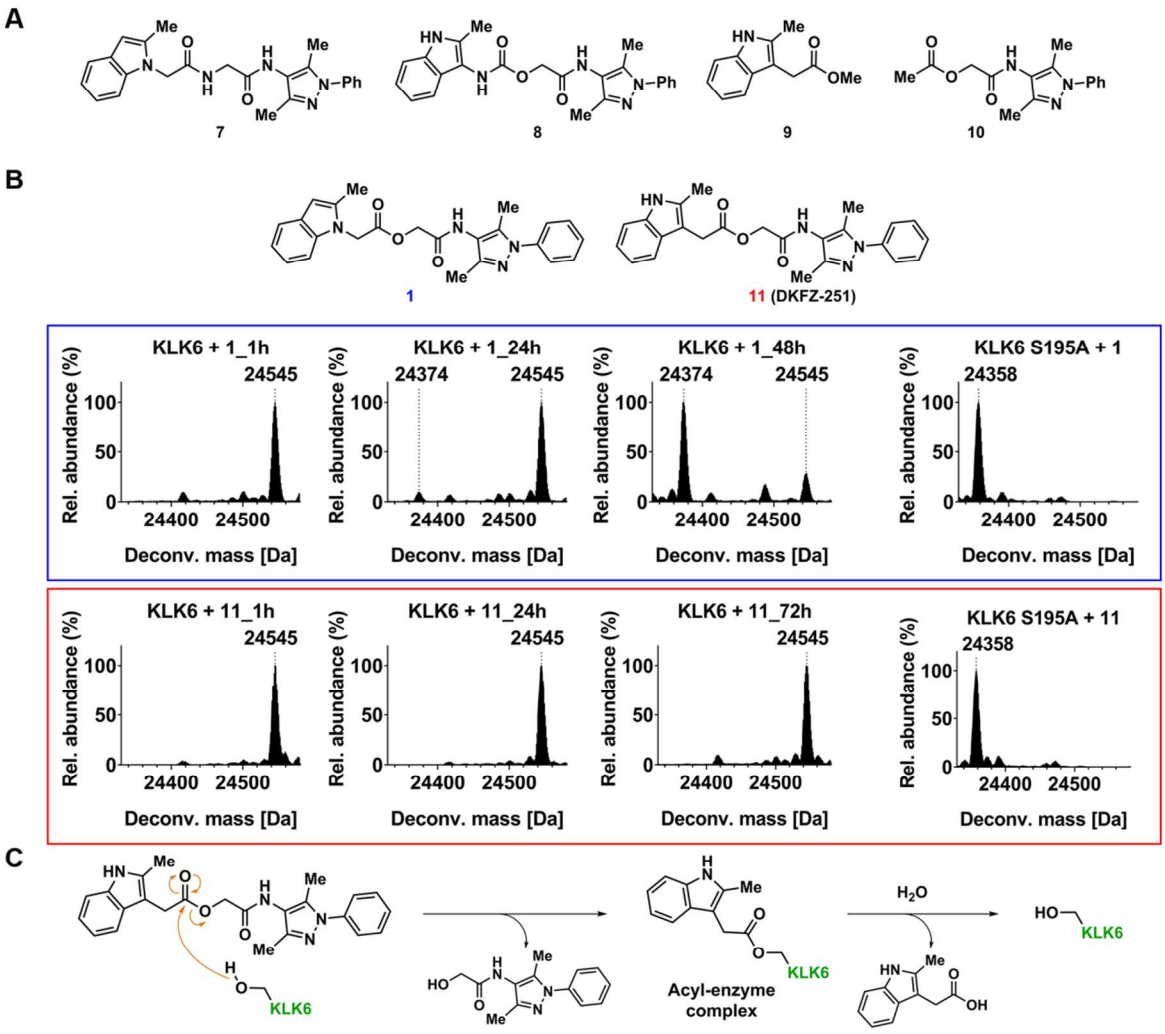

Figure 2. Depsipeptides are transient covalent inhibitors. (A) Structures of **7**–**10**. (B) ESI-MS of KLK6 (24,374 Da) treated with **1** or **11** (DKFZ-251) fully shifts the mass to 24,545 Da (ΔDa = 171) after 1 h. Longer incubation times show recovery of unmodified KLK6 with **1**, but not with **11**. An S195A mutant of KLK6 (24,358 Da) is neither modified by **1** nor **11**. (C) Reaction of **1** with the catalytic serine of KLK6, followed by the hydrolysis of the resulting acyl-enzyme complex.

Observation of the covalent adduct of **1** with KLK6 via intact protein MS at incubation times longer than 1 hour revealed that the covalent modification is transient. While the enzyme was still almost completely modified after 24 h, most of it was in an unmodified form after 48 h

(Figure 2B). Interestingly, the transient nature of the modification was found to be quite sensitive to changes in the western moiety structure. For example, regioisomer **11** (DKFZ-251) showed no recovery of native enzyme even after 72 h under the same conditions (Figure 2B).

These data indicate that the inhibitors act as substrate mimics, undergoing cleavage of the ester bond via nucleophilic attack by Ser195 to produce an acyl-enzyme complex that is resistant, but not impervious, to hydrolysis (Figure 2C). The fact that **1** exhibits selectivity for KLK6 over related serine proteases suggests that it is not simply a reactive, nonspecific affinity labeler. Moreover, the finding that both the western and eastern moieties are important for inhibition indicates that non-covalent interactions between the enzyme and inhibitor are required before reaction can occur. Taken together these results are consistent with the inhibitors acting via transient quiescent affinity labeling, as described by eq 1.

$$E + I \underset{k_{-1}}{\overset{k_1}{\rightleftharpoons}} E\text{–}I \xrightarrow{k_{on}} E\text{–}I^* \xrightarrow{k_{off}} E + I^* \quad (1)$$

First, equilibrium is rapidly (presumed) established between free enzyme (E) and inhibitor (I) with a non-covalent enzyme inhibitor complex (E-I) in a reversible manner. This step is guided by an intrinsic affinity of the compound to the KLK6 active site. Once brought into close proximity to the catalytic serine, the ester bond covalently reacts with KLK6, forming an acyl-enzyme complex (E-I*). This step is irreversible as the alcohol part of the ester is lost to the bulk solvent. The acyl-enzyme complex is hydrolyzed by water, after which, similarly to endogenous protein substrates, the corresponding carboxylic acid (I^*) is released. This step is also irreversible, as the acid is not able to bind again to KLK6 (data not shown). When the half-life of E-I* is long enough, the enzyme accumulates as E-I*, resulting in effective inhibition of the enzymatic function.

Structure–Activity Relationship Studies Reveal Strict Requirements for Effective KLK6 Inhibition

Having successfully elucidated the mechanism of action (MOA) of hit compound **1**, we set out to explore the structure–activity relationship (SAR) of this class of compounds with respect to its three components (W, L, and E, as defined in Figure 1B). We decided to utilize k_{inact}/K_I values as a metric to compare derivatives, working under the assumption that enzyme acylation would be essentially irreversible during such an experiment.[30] DKFZ-251 (**11**) behaved as expected, showing a time-dependency between residual enzyme activity and pre-incubation time of enzyme with inhibitor (Figure 3A). From this data, a k_{inact}/K_I of 1883 $M^{-1}s^{-1}$ (95% C.I. 1593 to 2172) could be determined (Figure 3B). When the same assay was performed with **1**, however, no time-dependency, up to a 40 min pre-incubation, was observed. When the pre-incubation time range was extended to 4 h, ester **1** appeared to "lose" potency over the assay time course (Figure 3C). By testing a larger panel of structures (Figures S6–8), we observed that for some compounds it was similarly inconclusive to measure k_{inact}/K_I. In the case of such substances, the half-life of E-I* is presumably too short to allow such a measurement. Unable to utilize k_{inact}/K_I values to compare all structures, we decided to utilize "apparent" IC_{50} values (referred to as IC_{50} from now on) after a relatively long pre-incubation time (30 min), as a compromise meant to capture as much of the relevant features of eq. 1 for each substance as possible.

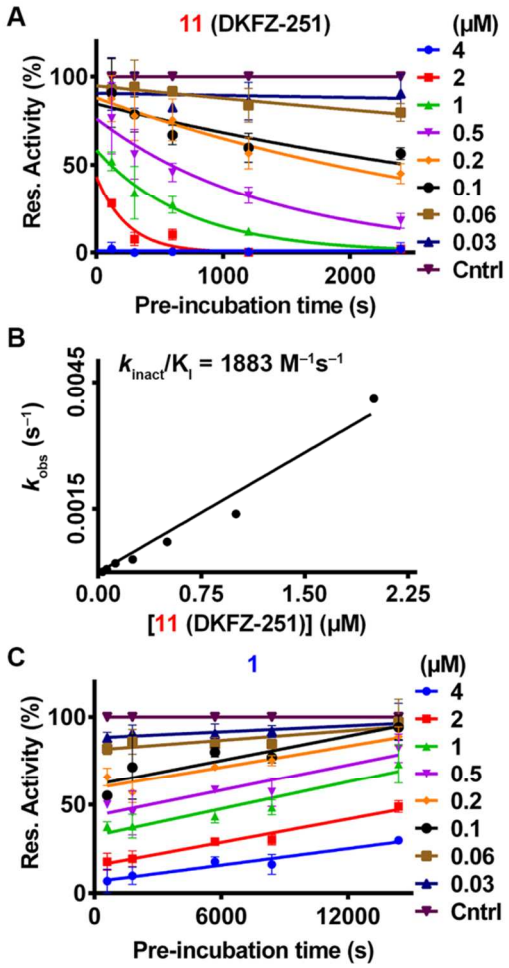

Figure 3. Time dependent behavior of **1** and **11** (DKFZ-251). (A) KLK6 residual activity after different pre-incubation times with, and at different concentrations of, **11**. (B) Plot for determination of k_{inact}/K_I for **11**. (C) KLK6 residual activity after different pre-incubation times with, and at different concentrations of, **1**. Residual activity in (A) and (C) was measured in triplicate at each time point and concentration. k_{obs} for each concentration in (A) was determined by fitting to an exponential decay function.

All compounds were tested against both KLK6 and trypsin in order to monitor selectivity. A steep SAR was identified for the W part of the molecule, as anticipated from the HTS, with indoles representing the best scaffold (Table 1). A switch in indole substitution from N-linked

(**1**) to C3-linked (**11**, DKFZ-251) resulted in an increase in potency of almost 5 fold. The free NH of **11** is required for potency as neither benzimidazole **12** nor N-methylindole **13** are comparable in potency (not even to **1**, hinting to both steric and electronic effects being important). Remarkable was the effect of the methyl group in the 2-position of the indole, the removal of which (**14**) decreased the activity relative to **11** more than 100 fold. The small methyl group seems to represent the best fit, as a larger isopropyl substituent (**15**) also strongly decreased potency. Further substitution of the indole with a chlorine atom produced moderate to significant potency losses (**16** and **17**, respectively). While substitution of indole in **11** for azaindole has little effect on KLK6 potency for 6- (**18**) and 7- (**19**) aza derivatives, it is moderately to extremely detrimental for activity at positions 5 (**20**) and 4 (**21**), respectively. Remarkably, the nitrogen in 7-azaindole **19** causes a dramatic loss of activity against trypsin relative to **11**, while 6-azaindole **18** loses almost all selectivity between the two enzymes. The basic nature of the introduced nitrogen may in fact start triggering interactions with the conserved Asp189 in the S1 pocket, and the placement of the nitrogen atom in **18** seems to be geometrically optimal (v. infra).

Table 1. Structure–activity relationship data

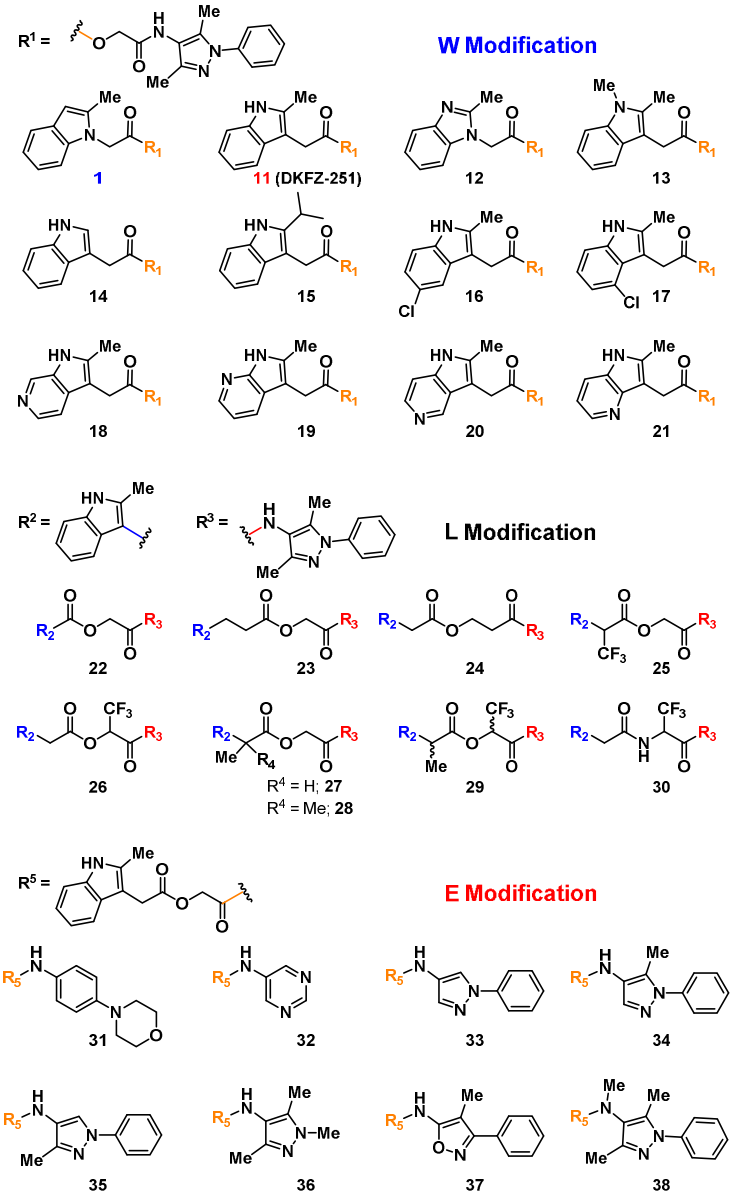

Cmpd	IC$_{50}$ (μM)[a]	
	KLK6	Trypsin
1	0.64 ± 0.29	38 ± 3
11	0.13 ± 0.04	21 ± 6
12	8.9 ± 4.3	>200
13	6.2 ±2.4	>200
14	15 ± 6	150 ± 25
15	13 ± 8	>200
16	0.25 ± 0.02	34
17	7.6 ± 1.4	>200
18	0.10 ± 0.05	0.33
19	0.19 ± 0.04	>200
20	0.49 ± 0.15	25
21	6.0 ± 3.9	61
22	>200	>200
23	58 ± 4	>200
24	110 ± 25	>200
25	23 ± 4	>200
26	0.018 ± 0.015	0.38
27	28 ± 2	>200
28	>200	>200
29	2.31 ± 0.04	61
30	>200	>200
31	4.4 ± 2.9	>200
32	17.0 ± 0.4	>200
33	6.99 ± 0.01	>50
34	0.29 ± 0.14	34
35	7.5 ± 3.2	>200
36	1.4 ± 0.1	>50
37	1.2 ± 0.6	50
38	2.8 ± 0.1	8.6 ± 0.6

[a] IC$_{50}$ values on KLK6 represent the mean of at least two independent experiments performed in triplicate ± standard deviation after 30 min pre-incubation; IC$_{50}$ values on trypsin represent the mean of at least one experiment performed in triplicate (± standard deviation when multiple independent experiments were performed) after 30 min pre-incubation.

The depsipeptidic scaffold (L) of DKFZ-251 (**11**) was explored in order to define the requirements for its structure and reactivity (Table 1). Deletion (**22**) or insertion (**23**) of a methylene between the indole and the ester resulted in inactive or significantly less potent

compounds, respectively. Moreover, the peptidomimetic nature of the depsipeptide was shown to be critical, as the introduction of a further methylene between the ester and the amide almost completely abolished activity (**24**). On the basis of the MOA elucidation, we next tried to enhance the compound potency by increasing the reactivity of the ester. An electron-withdrawing trifluoromethyl group was introduced on the carboxy (**25**) and on the alkoxy (**26**) part of the ester. Only the latter compound resulted in a potency increase, while **25** showed reduced potency that was comparable to the introduction of a simple methyl group (**27**). The di-methylated derivative **28** was found to be completely inactive. A hybrid substance (**29**), based on **26** and **27**, only somewhat counteracted the loss of potency given by the steric hindrance of the methyl group. The electron-withdrawing effect of the trifluoromethyl group was also not able to activate peptidic analogue **30** for KLK6 acylation. Altogether, these results suggest that inductive effects, which result in a better leaving group in E (e.g. **26**), can affect the compound potency by increasing its reactivity toward KLK6. On the other hand, steric hindrance of the ester (e.g. **27**), even when combined with inductively activating effects (e.g. **25**) reduces reactivity toward KLK6.

Complete substitution of the E part of DKFZ-251 (**11**) with other aromatic systems (e.g. 4-morpholinophenyl (**31**) or pyrimidine (**32**)) resulted in a significant loss of potency (Table 1). Thus, we started systematically investigating the different features of the highly substituted pyrazole ring. The methyl groups, which are suggestive of a constrained rotation for the amide and the N-phenyl bonds, are critical for KLK6 affinity, as shown by bis-demethylated **33**. Compounds **34** and **35** were synthesized to probe this effect, ascribing it mostly to the methyl in position 5. In fact, **34** was found to be only about 2-fold less active than **11**, while **35** was over 50 fold less potent and essentially equipotent to **33**. The phenyl ring also contributes to the

affinity to KLK6, and its substitution with a smaller methyl group (**36**) resulted in a 10-fold less potent inhibitor. Compounds bearing different 5-membered heterocycles such as isoxazole **37** were also found to be less potent, implying that the 5-methyl and the phenyl group in the absence of the pyrazole are not sufficient for retaining the affinity of **34** to KLK6. Finally, **38** showed that the presence of an NH in the peptidic bond seems to be required in order to interact with KLK6 (likely to build H bond interactions, typical of the peptidic substrate recognition), and it is intriguing albeit not fully clear to notice that **38** also has decreased selectivity toward trypsin. In summary, the E part of **11** plays an important role for inhibitor efficacy, in agreement with a 2-step inhibition mechanism, but in general the substances are still active if the 2-methyl-3-substitued indole is maintained in W.

Acyl-enzyme Complex Stability is Sensitive to Structural Changes

Given the inability to measure k_{inact}/K_I for all the different structures and having no means to directly measure k_{on}, we decided to measure k_{off}. KLK6 was incubated with an excess of inhibitor for 1 h, so that complete labeling of the enzyme was achieved (as observed in the ESI-MS experiments). Upon excess inhibitor removal (performed with desalting columns), immediate recovery of KLK6 enzymatic activity was observed for **1** as opposed to DKFZ-251 (**11**), where a $t_{1/2}$ of 6.43 h (95% C.I. 5.93–7.03) was measured (Figure 4). While consistent with the k_{inact}/K_I measurements (see Figure 3), the difference in $t_{1/2}$ values is surprising for such an apparently small change in the structure. A potential explanation for this difference is that the indole N-linkage of **1** tends to decrease the stability of the acyl-enzyme ester intermediate toward water hydrolysis via inductive electron-withdrawing effects, while the indole C3-linkage in **11** tends to inductively increase the stability of the acyl-enzyme intermediate due to the relatively high electron density found at C3 of an indole. Also surprising is the fact that **14**, which differs from

11 only by the lack of an indole C2 methyl group, produced an acyl-enzyme intermediate with a half-life shorter than 10 min. This suggests that a combined effect of the C2 methyl group (which presumably increases acyl-enzyme stability through steric hindrance, but also potentially through electron-donating effects) and the substitution pattern of the indole ring, is responsible for the stability seen with **11** in comparison to structurally related **1** and **14**. For the acyl-enzyme intermediate formed from **27**, KLK6 enzymatic activity was not fully recovered within the experiment timescale (predicted $t_{1/2}$ = 19.1 h, 95% C.I. 16.1–23.4). Notably, **33** which has a much lower potency (higher IC_{50} value) than **11**, but bears an identical W group, was found to give a similar acyl-enzyme stability profile, consistent with only W influencing this step of the inhibition mechanism. The lower IC_{50} of **33** likely results from decreased affinity to the KLK6 active site in the first reversible recognition step. Although **27** forms the longest-lived covalent adduct with KLK6, its higher IC_{50} value relative to **11** (likely due to a smaller k_{on}) renders it less suitable for use as a chemical probe. Altogether DKFZ-251 (**11**) is the best candidate to probe KLK6 as it exhibits a balance between rapid on-rate coupled with a long lived acyl-enzyme complex.

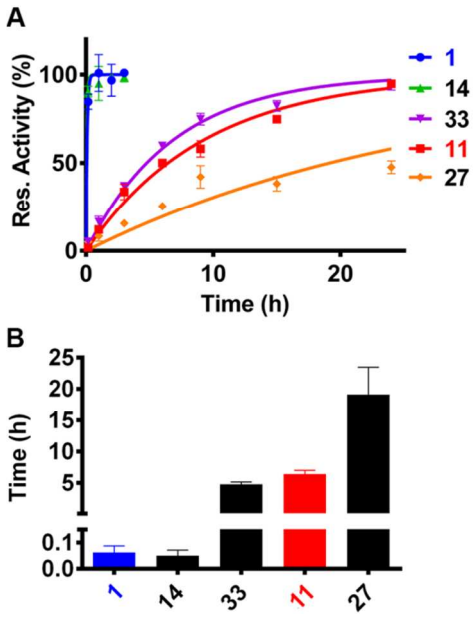

Figure 4. Acyl-enyzme complex stability determinations for a panel of selected inhibitors. (A) Aliquots from a solution of acyl-enzyme complex, after excess inhibitor removal, were tested in triplicate at different time points (10 min, 1 h, 2 h and 3 h for **1** and **14**, and 10 min, 1 h, 3 h, 6 h, 9 h, 15 h and 24 h for **33**, **11** and **27**) by addition of FSR-AMC and fluorescence detection at 25 °C. Data were fit to an exponential growth equation, which was used to calculate half-life values. The values are shown in (B) (± standard deviation).

Docking Studies are Supported by the Synthesis of Amidine Derivatives

Intrigued by the lack of a clearly basic moiety that could act as a P1, we performed a docking study to analyze the most important interactions within the KLK6 active site. A restricted docking of DKFZ-251 (**11**) was performed using a previously solved crystal structure of KLK6 (PDB: 4D8N), and a model of the tetrahedral intermediate formed between Ser195 and **11** was built (Figure 5A, Figure S9). In this model, the amide bond of DKFZ-251 (**11**) engages in an H-bond with L41 in the surroundings of the S1' pocket, an interaction that is consistent with somewhat structurally related compounds co-crystallized with KLK7.[31] In addition, the indole occupies the S1 pocket and the negatively charged oxygen of the tetrahedral intermediate is stabilized in the canonical oxyanion hole, where it is coordinated by the backbone N-Hs of S193 and Ser195 in two bridged H-bonds. A previously reported KLK6 crystal structure with a non-covalent inhibitor (PDB: 3VFE) indicates a lipophilic interaction of the P1 group with I218, which could also be made by the indole ring of DKFZ-251 (**11**) (Figure S10).[21b] This amino acid is less conserved in serine proteases and could at least partially account for the selectivity shown by **11** for KLK6 against other proteases such as trypsin. Superimposing the tetrahedral intermediate pose with the crystal structure of KLK6 in complex with benzamidine (PDB: 1L2E) suggested that the introduction of an amidine moiety in the indole ring of **11**, specifically at the

6, but not the 5, position, would enable H-bond interactions with Asp189. To test this hypothesis, we synthesized **39** and **40** (Figure 5B), bearing an amidine in positions 6 and 5, respectively.

As predicted, **39** is highly potent against KLK6, reaching the IC_{50} assay limit of 2.5 nM, while **40** is essentially equipotent with DKFZ-251 (**11**). Interestingly, **39** proved to also be a highly potent inhibitor of trypsin ($IC_{50} \leq 1$ nM), while **40** showed only a slightly improved potency against trypsin relative to **11**, implying that the amidine in position 6, but not 5, of the indole can engage in the Asp189 H-bond network, similarly to canonical basic P1 groups used for trypsin-like serine proteases inhibitors. The peptidic analog of **39**, bis-amide **41** (Figure 5B), was found to be a reasonably good KLK6 inhibitor ($IC_{50} = 1.2 \pm 0.4$ μM), but selectivity over trypsin was lost, thus supporting the notion that polar basic P1 residues, if correctly placed, make strong interactions with the S1 pocket of both KLK6 and trypsin. These data are consistent with the specific MOA of the inhibitor class being critical for their selectivity as well.

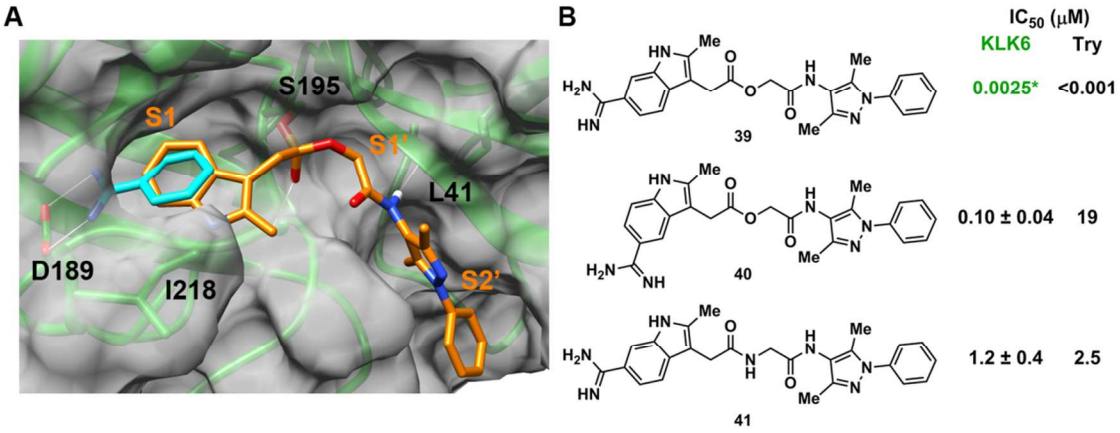

Figure 5. Docking studies and inhibition data of amidine-containing derivatives. (A) Covalent docking of KLK6 (light green, PDB: 4D8N) with DKFZ-251 (**11**) (orange) superimposed with KLK6 (hidden) co-crystallized with benzamidine (turquoise, PDB: 1L2E). H-bonds given by each compound are shown (white). (B) Structures and IC_{50} values of amidine derivatives **39–41**.

KLK Sub-type Selectivity Screening

Aware of the high degree of homology amongst tissue-kallikreins, we tested DKFZ-251 (**11**) against a panel of 6 other KLKs (KLK4, 5, 7, 8, 13, and 14 – see Experimental Section for details on the production and purification of these enzymes). Intrigued by the effect of the amidino group in position 6 of the indole, **39** was also tested (Table 2). In these assays the compounds were pre-incubated with the enzymes for 10 min, giving as expected slightly higher IC_{50}s against KLK6 than in Table 1. KLK7 has chymotryptic-like specificity, and recognizes non-basic P1 residues as substrates, but both **11** and **39** are much less active against KLK7 as compared to KLK6. DKFZ-251 (**11**) shows KLK6 selectivity against KLK4 (>400 fold), and KLK8, KLK13, and KLK14 (all three >20 fold). On the other hand, selectivity is partially retained by **39** against KLK8 (9 fold) and KLK13 (>20 fold), but not in the case of KLK14. KLK5, which is very similar in structure and active site shape to its cognate KLK6, is the second favored target of **11** with only about a 2 fold difference in activity relative to KLK6, while **39** is about 6 fold less active. The selectivity of **11** against secreted serine proteases (Figure S11) and recombinant KLKs (Figure S12) was also tested in a more complex environment (derived from conditioned cell culture medium) using broad spectrum activity-based probes to visualize the proteins by in-gel fluorescence. At concentrations as high as 50 μM, pre-incubation with **11** only prevents probe binding to KLK6, leaving the other protease levels unchanged.

Table 2. KLK selectivity screen of **11** and **39**.

Enzyme	IC_{50} (μM)[a]	
	11 (DKFZ-251)	**39**
KLK4	>200	N.M.[b]
KLK5	1.1 ± 0.5	0.130 ± 0.002
KLK6	0.47 ± 0.14	0.023
KLK7	73	>0.50
KLK8	>10	0.21
KLK13	>10	>0.50
KLK14	10.3 ± 0.3	0.008 ± 0.001

[a]Data represent the mean of at least one experiment performed in triplicates (± standard deviation when multiple independent experiments were performed) after 10 min pre-incubation of inhibitor and enzyme. [b] N.M. = not measured.

Compound Stability Correlates with Acyl-Enzyme Complex Stability

Compound stability toward ester hydrolysis in cell culture medium at 37 °C was measured as a means to assess the suitability of the compounds for cellular assays (Figure 6A). DKFZ-251 (**11**) demonstrated an increased stability profile in comparison to hit **1** with a half-life almost 8 times longer ($t_{1/2}$ = 4.22 h, 95% C.I. 4.01–4.44, and 0.56 h, 95% C.I. 0.54–0.59, respectively). Interestingly **14**, which lacks the 2-methyl group of **11**, was rapidly hydrolyzed ($t_{1/2}$ = 0.45 h, 95% C.I. 0.44–0.46), while, as expected, steric shielding with an additional methyl group (**27**) stabilized the ester, ($t_{1/2}$ = 15.2 h, 95% C.I. 13.7–17.1). The chemical stabilities of **1**, **11**, **14**, and **27** closely parallel the stabilities of the corresponding acyl-enzyme complexes which they produce (see Figure 4), suggesting that the acyl-enzyme complex lifetimes are governed by the intrinsic chemical properties of the inhibitor structure, and don't involve non-covalent interactions with the enzyme. Inductive activation of the ester results in rapid hydrolysis, e.g**. 26** ($t_{1/2}$ = 0.425 h, 95% C.I. 0.420–0.430), and **29**, which combines the stabilizing methyl group of **27** with the destabilizing trifluoromethyl group of **26**, gives an intermediate stability profile ($t_{1/2}$ = 1.68 h, 95% C.I. 1.60–1.73). Interestingly, amidine **39** also shows a less stable profile ($t_{1/2}$ = 1.32 h, 95% C.I. 1.16–1.52), which might result from combined increased proteolytic

cleavage of the ester bond (due to its lower selectivity profile) in addition to water hydrolysis. Substance **40**, which also contains an amidine group, does show a decrease in stability compared to **11**, but not as dramatic ($t_{1/2}$ = 2.88 h, 95% C.I. 2.57–3.26), in agreement with its retained selectivity.

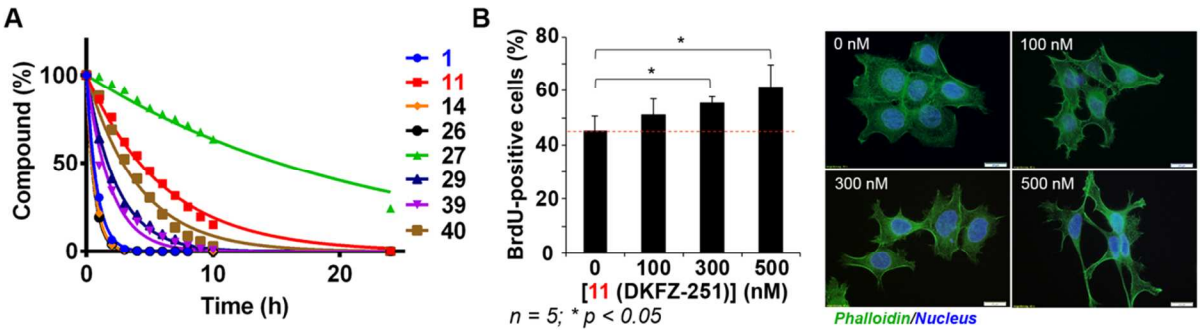

Figure 6. (A) Stability of a selection of compounds in DMEM at 37 °C. (B) *In vitro* results of DKFZ-251 (**11**) on FaDu cells after a daily treatment for 48 h. Both proliferation (measured via BrdU incorporation) and phenotypic EMT are affected by **11** in a dose-dependent fashion as previously reported for KLK6 shRNA.[17] BrdU incorporation results are the average from 5 independent experiments ± standard deviation.

Cellular Assay Demonstrates On-Target Activity

To assess the activity of the KLK6 inhibitors in cells we used a recently published phenotypic assay, which correlates the expression of KLK6 in FaDu cells to proliferation and morphology.[17] In this assay, a daily treatment of FaDu cells for 48 h with DKFZ-251 (**11**) (Figure 6B), but not with inactive carbamate analogue **8** (Figure S13), copied the shRNA-mediated KLK6 silencing phenotype in a dose-dependent fashion. The same effect was not triggered in other head and neck tumor cell lines (Cal27, Detroit562), which do not express high basal KLK6 levels and do not show growth- and morphological-dependence to this protein (Figure S14). These data indicate that DKFZ-251 (**11**) is able to effectively inhibit endogenous KLK6 in a cellular context.

Development of Inhibitor-based ABPs for Research Application

Having validated the MOA, selectivity profile, and cellular activity of the substance class, we utilized the scaffold of DKFZ-251 (**11**) to develop activity-based probes (ABPs). Distinguishing active from inactive KLKs[32] (and proteases in general) in tissue-derived samples is highly desirable as it could enhance the prognostic value of KLKs as biomarkers.[33] Moreover ABPs are powerful tools with wide applicability in basic research and drug discovery.[34] To functionalize our inhibitors for ABP development, an alkyne was introduced in the W part of the structure via Sonogashira coupling, and 4 derivatives were synthesized (**42–45**, Figure 7A). These showed SAR in accordance with previous results; notably, **43** has excellent selectivity against trypsin. DKFZ-633 (**44**), which showed the best labeling in a preliminary assay, was chosen for further validation. The probes were initially tested in concentrated conditioned medium from the KLK3-rich LNCap cell line, to which recombinant KLK6 was added.[35] After incubation with the probe, and copper-catalyzed alkyne–azide cycloaddition (CuAAC) with a TAMRA-labeled azide, the samples were visualized "in-gel". DKFZ-633 (**44**) selectively labeled KLK6 at all probe concentrations tested and within a 10 min incubation (Figure S15). Encouragingly, the labeling was persistent up to 6 h and resistant to the denaturing conditions used. Labeling of KLK6 (10 µM **44**, 1 h incubation) was inhibited in a dose-dependent fashion by pre-incubation for 30 min with **11** but not inactive analog **8** (Figure 7B). Optimized conditions (2.5 µM, 1 h incubation) were then used to determine the efficiency of KLK6 detection, with **42** and **44** being able to detect KLK6 at levels as low as 0.05% of the total protein in the sample (Figure S16). Finally, by utilizing a biotin-labeled azide as an enrichment handle, we were able to pull down endogenous KLK6 in a dose-dependent fashion in FaDu cell conditioned medium (Figure 7C). Encouraged by these results we also tested the activity of KLK6 in cell culture medium from a panel of cell

lines, and interestingly found that the amount of active protein does not correlate to its relative abundance (Figure 7D), for example in SCC9 cells. Interestingly, two glycoforms of KLK6,[36] which showed cell-dependent relative abundance, could be enriched with DKFZ-633 (**44**).

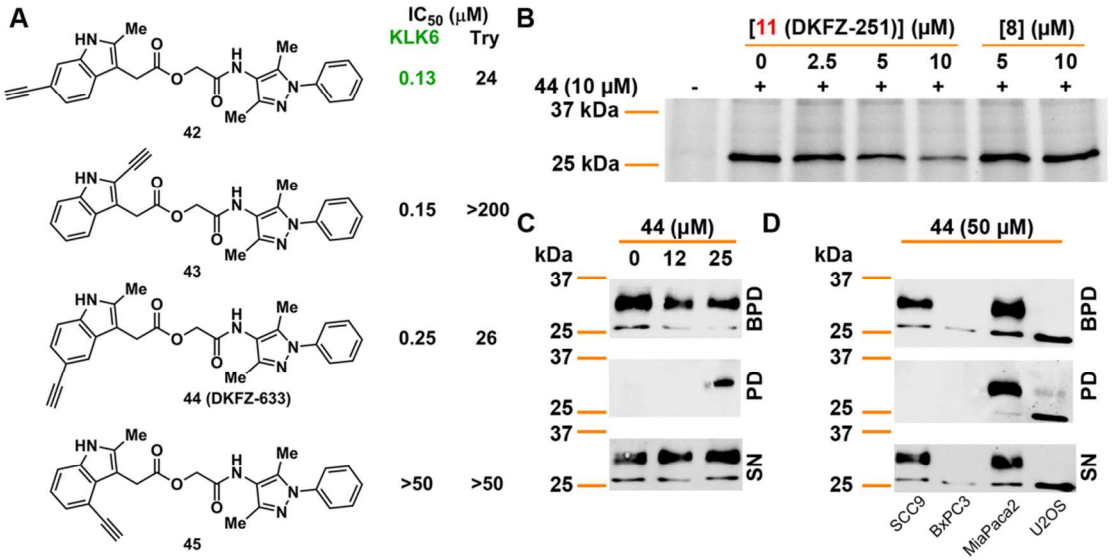

Figure 7. Activity-based probe studies. (A) Structure and IC_{50} values (30 min pre-incubation) of **42–45**. (B) In-gel fluorescent labeling of KLK6 (60 ng in 20 μg total protein) by **44** (after CuAAC with a TAMRA-labeled azide) is prevented by prior incubation with parent inhibitor **11**, but not by inactive carbamate **8**, in a dose-dependent fashion. (C) Western blot of endogenous KLK6 pulled down by **44** (after CuAAC with a biotin-labeled azide) in conditioned FaDu cell medium shows dose-dependent behavior. (D) Western blot of active KLK6 pulled down from different cell line conditioned medium. BPD: aliquots from the total mixture before the pull down; PD: pull down samples; SN: aliquots from the supernatant after the pull down.

Chemical Synthesis

The preparation of most of the substances in this study is depicted in Scheme 1. For the synthesis of substances with an N-phenyl-3,5-dimethyl-2-aminopyrazole E group, 3,5-dimethylpyrazole (**46**) was converted to highly substituted pyrazole **47** via a three step

nitration/N-arylation/reduction sequence. Amide formation with acid **48**, or with acid chloride **49** (which gave **10**, see Figure 2) followed by acetate removal, gave alcohols **51** and **50**, respectively. The critical ester bond could then be formed with a variety of different substituted carboxylic acids. For compounds with a 2-methyl-3-acetylindole W group, acid **52** was condensed with benzyl glycolate (**53**) to give ester **54**. After hydrogenolysis of **54** to give acid **55**, amide coupling with various primary amines proceeded to give final inhibitors for testing. Substances **7**–**9**, **24**, **30**, **33**, **38**, and **41** required slightly different preparations, which are detailed in the supporting information.

Scheme 1. General synthetic scheme toward depsipeptide KLK6 inhibitors[a]

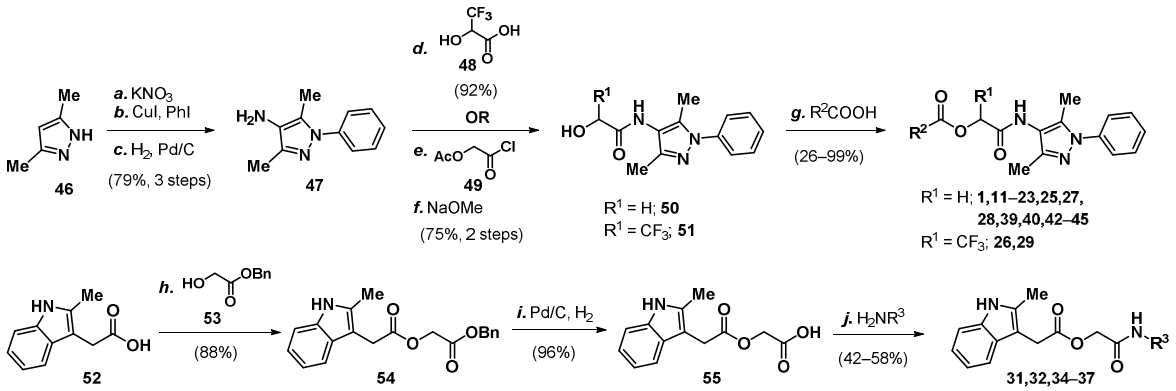

[a]Reagents and conditions: (a) KNO_3 (1.6 equiv), H_2SO_4, 100 °C, 18 h, 83%; (b) CuI (5 mol%), PhI (3.7 equiv), *trans*-N,N´-dimethylcyclohexane-1,2-diamine (20 mol%), 180 °C (microwave), 4 h, 96%; (c) H_2 (4 atm), 10% Pd/C, EtOH/$CHCl_3$ 7:1, r.t., 48 h, quantitative; (d) **48** (1 equiv), DCC (1.2 equiv), *i*-Pr_2Net (1.2 equiv), MeCN, r.t., 24 h, 92%; (e) **49** (1.2 equiv), Et_3N (1.5 equiv), –10 °C, 5 h, 78%; (f) NaOMe (3 mol%), MeOH, r.t., 3 h, then HCl, 96%; (g) R^2CO_2H, DCC or EDCI, *i*-Pr_2NEt, DMAP, MeCN or CH_2Cl_2 or THF, r.t., 26–99%; (h) **53** (1 equiv), DCC (1 equiv), DMAP (0.2 equiv), CH_2Cl_2, r.t., 4 h, 88%; (i) H_2 (1 atm), 10% Pd/C, EtOAc, r.t., 48 h, 96%; (j) R^3NH_2, DCC, EDCI, or HATU, *i*-Pr_2NEt, CH_2Cl_2 or THF, r.t., 42–58%.

The preparation of **39** and **40** is of note, as it required the synthesis of compounds containing a polar amidine group in the presence of an ester. Amidines are often prepared from the corresponding cyano derivative by reaction with hydroxyl amine and then reductive cleavage of

the N-O bond. Both reactions require relatively harsh conditions, which would normally not be compatible with an ester. Moreover, the intermediates and products in such a reaction sequence are typically very polar and can be challenging to purify. Our approach to **39** and **40** circumvents these problems by revealing the polar amidine in the final step, and the synthesis of **39** is depicted in Scheme 2. Fischer indole synthesis using 3-bromophenylhydrazine (**56**) and 4-oxopentanoic acid (**57**) in EtOH gave bromide **58**, which was converted to boronic acid **59** via Miyaura borylation. The fully protected amidine was installed with a modified Liebeskind–Srogl coupling of **59** and pseudothiourea **60**.[37] The resulting amidinoindole (**61**) was saponified to give acid **62**, which was then coupled with alcohol **50** to give ester **63**. TFA-mediated deprotection then provided amidine **39**. The synthesis of **40** proceeded analogously.

Scheme 2. Synthesis of amidine **39**[a]

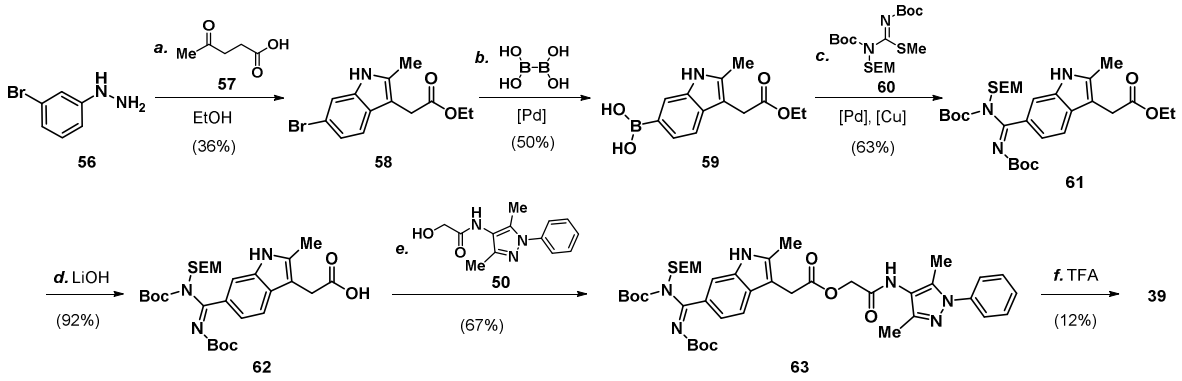

[a]Reagents and conditions: (a) **57** (1 equiv), H_2SO_4, EtOH, reflux, 66 h, 36%; (b) tetrahydroxydiboron (1.5 equiv), Xphos Pd G2 (1 mol%), XPhos (2 mol%), KOAc (3 equiv), NaO*t*-Bu (1 mol%), EtOH, 80 °C, 16 h, 50%; (c) **60** (1 equiv), Pd_2dba_3 (5 mol%), CuTC (3 equiv), TFP (35 mol%), THF, 70 °C, 17 h, 63%; (d) LiOH, dioxane/DMF/water 4:2:1, r.t., 18 h, 92%; (e) **50** (0.9 equiv), EDCI (2 equiv), DMAP (0.2 equiv), CH_2Cl_2, r.t., 18 h, 67%; (f) 1:5 TFA/CH_2Cl_2, r.t., 5 h, 12%.

CONCLUSIONS

Despite continuing reports that KLK6 plays an important role in different pathologies, the molecular mechanisms by which it affects cancer and neurodegenerative diseases is not yet fully

understood. Indeed, the lack of selective and potent inhibitors has slowed down the progression of such studies, limiting target validation tools to protein silencing and overexpression, with no pharmacological means to investigate what role KLK6 enzymatic activity plays in disease. To the best of our knowledge, we report here the first class of inhibitors suitable for investigating the biology of KLK6. The compounds are potent and selective within the tissue kallikrein family as well as related proteases, and they inhibit KLK6 via transient quiescent affinity labeling. The inhibitors must contain an ester bond for reactivity, and this ester bond is susceptible to water hydrolysis. The intermediate which is formed after reaction of an inhibitor with the enzyme also undergoes hydrolysis, and the relative stabilities of the parent esters and their resulting acyl-enzyme intermediates correlate. An appropriate balance between rapid reactivity and long lasting inhibition is therefore required for an effective inhibitor. Potency is also modulated by non-covalent interactions that govern the initial affinity for the inhibitor toward the enzyme, and which have no effect on the acyl-enzyme complex lifetime. On the other hand, incorporation of a basic P1 residue, correctly placed to interact with Asp189 in the S1 pocket of KLK6, was found to increase this initial affinity, but was detrimental for selectivity. Our data show that DKFZ-251 (**11**) presents the best balance of KLK6 activity, selectivity, and stability, and is an effective chemical probe for cellular experiments, as demonstrated in a phenotypic assay with FaDu cells. Moreover, we exploited the inhibition MOA to develop ABPs, which were validated via “in-gel” fluorescence experiments. The best ABP, DKFZ-633 (**44**), was used to pull down active endogenous KLK6 from conditioned medium in a variety of different cell lines. We preliminarily found that two cell lines, while containing KLK6, had no active enzyme. The probes should be suitable also for use on patient-derived samples. We envision that this new class of compounds

together with the generated ABPs will help advance our understanding of the physiological and, importantly for translation, pathological role of KLK6.

EXPERIMENTAL SECTION

Chemical Synthesis

All organic synthesis experiments were performed in solution under air unless otherwise specified. Reagents and solvents were purchased from Sigma Aldrich, Santa Cruz, VWR, EnzoLifeSciences and AlfaAesar and used without purification. Anhydrous CH_2Cl_2, toluene, MeCN and THF were prepared with an MBraun SPS800 Solvent Purification System. Thin layer chromatography (TLC) was carried out on Merck glass silica plates. TLC visualization was accomplished using 254 or 366 nm UV light or charring solutions of $KMnO_4$, cerric ammonium molybdate, or *p*-anisaldehyde. Purification was performed by flash column chromatography using SiliCycle SiliaFlash® P60 (40–63 µm, 60 Å particle size) or via RP-HPLC (Agilent 1260 Infinity and an ES quadrupole Agilent 6120, column: Kinetex® 5µm C18 100 Å, AXIA Packed LC Column 250 x 21.2 mm; Temperature = 40 ºC; Solvent A = H_2O, 0.05% TFA; Solvent B = MeCN, 0.05% TFA; Flow Rate = 15.0 mL/min; method: Gradient: 95% A → 70% A [over 4 min], then 70% A → 40% A [over 8 min], then 40% A → 5% A [over 4 min]).

Analytical LC/MS was performed on an Agilent 1260 Infinity system using reverse phase. Column: Kinetex® 2.6 µm C18 100 Å, LC Column 50 x 2.1 mm; Temperature = 40 ºC; Solvent A = H_2O, 0.01% HCO_2H; Solvent B = MeCN, 0.01% HCO_2H; Flow Rate = 0.60 mL/min; method: Gradient: 99% A → 10% A [over 6 min] then 10% A → 1% A [over 2 min]). High resolution mass spectrometry was recorded on a Bruker ApexQe FT-ICR instrument, (Organic Chemistry Institute, University of Heidelberg). NMR spectra were recorded on Bruker 400 MHz or 600 MHz instruments at 298.1 K. Melting points were determined on a semi-automated

apparatus (MPM-H2, Coesfeld Materialtest). All final compounds were found to have ≥ 95% purity, controlled by analytical (HPLC/UV/ELSD/MS) with the above described method, and confirmed by ^{1}H NMR.

Detailed synthesis procedures, characterization data, and NMR spectra can be found in the Supporting Information.

Protein Production and Purification

Trypsin was purchased from Polymun scientific. Thrombin was purchased from Biopur. Factor Xa was purchased from Enzo Life Sciences.

Recombinant KLK6. Recombinant KLK6 (R74G, R76Q, and N132Q)[21b] and KLK6 S195A (R74G, R76Q, and N132Q) proteins were produced as previously described[38] with minor changes. A pFastBac™ donor plasmid including cDNA encoding the sequence for the mature form of KLK6 and KLK6 S195A (both with additional R74G, R76Q, and N132Q mutations) preceded at 5´ from the gp64 signal peptide, a 6x His-tag and an enterokinase (EK) recognition sequence of $(Asp)_4Lys$ was purchased from Life Technologies™. This system was transformed in competent *E.coli* DH10MultiBac by electroporation. Transformed cells were grown overnight at 37 °C in 2x TY medium. 5 µL of 1:10 and 1:100 dilution of these cells were cultured on selection plates [YTE Agar + Carbenicillin (100 g/ml), Kanamycin (30 µg/ml), Gentamycin (7 µg/ml), Tetracycline (10 µg/ml), X-gal (400 µg/ml) and IPTG (5 mM)]. White colonies were re-streaked for monoclonal growth on the same plates overnight at 37 °C. Seven white cultures thus obtained were grown in a 3 mL culture for 24 h at 37°C in 2x TY supplemented with the above-mentioned antibiotics. Bacmid DNA containing the KLK6 constructs was isolated using Qiagen's miniprep kit following producer instructions and sequenced. DNA concentrations were determined using NanoDrop spectrophotometer (Thermo Scientific, MA, USA) and the construct

was stored at 4 °C prior to use. Sf21 cells were seeded in 6-well plates at 6 x 10^5 cells in 2 mL sf-900 II serum-free media (Gibco, Thermo Fisher) per well and let 15 min for adherence. To a mixture of FuGENE® (Promega) in medium was added each Bacmid construct separately and incubated 15 min at rt. 116 µL of this mixture was added to each well (constructs were added in duplicates) and cells were cultured at 27 °C for 48–60 h. V_0 viral stock obtained from this culture cycle was used to produce high titer V_1 stock from a new culture cycle in Sf21 cells cultured for 2 days after growth arrest (which was also used to test the protein expression on a small scale). The TniHi5 insect cell line was used for production of expressed protein by the viral stock and grown in Express Five™ SFM (Gibco, Thermo Fisher) for 72 h after cell cycle arrest. Cell culture supernatant was collected, filtered and loaded on an ÄKTA™ protein purification system loaded with a prepacked 5 mL cOmplete™ His-Tag Purification Column (Roche) equilibrated with 50 mM Tris/HCl, 250 mM NaCl pH 8.0. Flow-through was discarded and the protein was eluted from the column using 300mM imidazole elution buffer. Fractions containing protein as analyzed by SDS-PAGE were pooled and incubated overnight with 100 µL enterokinase, dializing in 1 L 50 mM Tris/HCl, 250 mM NaCl pH 8.0 buffer at 4 °C. The obtained solution was again purified with 5 mL cOmplete™ His-Tag Purification Column collecting the flow-through which contains the active KLK6 protein construct deprived of the His-tag. Fractions containing protein as analyzed by SDS-PAGE were pooled and dialyzed overnight with 1 L 50 mM Tris-HCl, 50 mM NaCl pH 7.0 buffer. The protein of interest was further purified by ion-exchange chromatography (5 mL HiTrapQ, 50 mM Tris-HCl, 1 M NaCl pH 7.0 elution buffer) followed by size exclusion chromatography (Superdex 75 10/300 GL, Aldrich®, 50 mM Tris-HCl, 50 mM NaCl pH 7.0 buffer). Final protein purity was determined by SDS-PAGE and ESI-MS, the protein concentration was determined by Bradford assay.

Recombinant pro-KLK4. Pro-KLK4 protein was produced in yeast with the following procedure. The *pro-KLK4* gene was amplified with overhangs containing primers "KLK4 to pPic9k" Fwd and Rev (see Supporting Information) and were cloned into *pPIC9K* expression vector (Invitrogen) using Gibson Assembly Master Mix kit (New England Biolabs) according to the kit protocol. With this method, a FLAG-tag was added to the N-terminus of the purified protein, and a His tag to the C-terminus. The product was electroporated into *E.coli*, incubated at 37 °C with shaking at 250 rpm for 1 h in LB medium [1% yeast extract (w/v), 2% peptone (w/v), and 2% dextrose (w/v)], plated onto LB-Amp plates (1 mg ampicillin/L), and incubated at 37 °C for 24 h. Several colonies were scraped from the plate, transferred into LB-Amp medium, and incubated at 37 °C with shaking at 250 rpm for 24 h. *pPIC9K* plasmids containing the *pro-KLK4* clones were isolated from each *E.coli* colony using HiYield plasmid mini-kit (RBC Bioscience, Taiwan) and were sequenced using "AOX1" Fwd and Rev primers (see Supporting Information). *pPIC9K* plasmids containing *pro-KLK4* clones with the correct sequence were linearized using SacI, and about 30 μg of DNA was electroporated into *P. pastoris* strain GS115 (Invitrogen, CA, USA) for chromosomal incorporation by homologous recombination. Transformed cells were plated onto RDB plates [18.6% sorbitol (w/v), 2% agar (w/v), 2% dextrose (w/v), 1.34% yeast nitrogen base (w/v), 4× 10–5 % biotin (w/v), and 5× 10–3 % of L-glutamic acid, L-methionine, L-leucine, L-lysine, and L-isoleucine (w/v)] and incubated for 3 days at 30 °C. Cells were scraped from the plates using E-buffer [0.12% Tris base (w/v), 9.24% sucrose (w/v), and 0.02% $MgCl_2$ (w/v; pH 7.5)] and plated onto YPD-G418 plates (4 mg/mL G418) for an additional 3 days. Colonies were harvested (about 10), seeded into 5 mL of BMGY medium [2% peptone (w/v), 1% yeast extract (w/v), 0.23% $K_2H(PO_4)$ (w/v), 1.18% $KH_2(PO_4)$ (w/v), 1.34% yeast nitrogen base (w/v), 4 × 10–5 % biotin (w/v), and 1% glycerol (v/v)], and incubated at 30 °C with shaking

at 300 rpm for 24 h. The *pro-KLK4* clone was analyzed for expression. For expression, cells from the BMGY medium were re-suspended in 5 mL of BMMY medium [2% peptone (w/v), 1% yeast extract (w/v), 0.23% K_2HPO_4 (w/v), 1.18% KH_2PO_4 (w/v), 1.34% yeast nitrogen base (w/v), 4×10^{-5} % biotin (w/v), and 0.5% MeOH (v/v)] to reach an OD600 of 1 and incubated at 30 °C with shaking at 300 rpm for 72 h, with 0.5% MeOH being added every 24 h. Protein expression and secretion to the media were analyzed by Western blot, using mouse anti-FLAG primary antibody (Sigma Aldrich) and alkaline phosphatase-conjugated anti-mouse secondary antibody (Jackson ImmunoResearch). BCIP reagent (Sigma Aldrich) was used for protein expression signal analysis according to the product protocol. Individual clones with the strongest expression levels were selected and subjected to large-scale expression. Briefly, clones in 1 mL of BMGY medium at an OD600 of 8–10 were added to 50 mL of BMGY medium at 30 °C with shaking at 300 rpm for 24 h. Cells were precipitated from the medium and induced for protein secretion in 500 mL of BMMY at 30 °C with shaking at 300 rpm for 72 h. MeOH (0.5%) was added every 24 h. After induction, the supernatant was filtered through a 0.22 μm vacuum filter. The filtrate was then subjected to the following workup: NaCl was added to reach a final concentration of 300 mM, imidazole (Sigma Aldrich) was added to give a final concentration of 10 mM, and the solution pH was adjusted to 8.0. After 1 h at 4 °C, the medium was filtered again, and the protein of interest was purified using 5 mL of Ni-NTA Sepharose beads column (Invitrogen). Ni-NTA beads column washed with 20 mL wash buffer and the remaining bound activated KLK4 protein was eluted from the Ni-NTA beads with 15 mL of elution buffer [PBS, 300 mM imidazole]. The eluted protein was concentrated to 5 mL using Vivaspin with a 5-kDa cutoff (Vivaproducts) and was then subjected to gel-filtration chromatography on a Superdex™ 75 16/600 GL column using an ÄKTA™ Pure (GE Biosciences) chromatography system. The

gel-filtration column was pre-equilibrated with PBS, and the protein was eluted with PBS buffer. Protein concentration was calculated from protein absorbance at 280 nm (extinction coefficient of 31,690 M^{-1} cm^{-1} and calculated mass of 25.3 kDa) obtained using a NanoDrop spectrophotometer (Thermo Scientific). Protein samples were also subjected to mass spectrometry analysis (Ilse Katz Institute for Nanoscale Science Technology, BGU). The purified protein was stored at –80 °C.

Other recombinant KLKs. Recombinant KLK5, KLK7, KLK8, KLK13, and KLK14 were produced using the Easyselect™ *Pichia pastoris* expression system (Invitrogen) as described in detail elsewhere.[39] KLKs were purified to homogeneity (> 95% purity on Coomassie Blue-stained polyacrylamide gels), and their identities were confirmed by tandem mass spectrometry.

Biochemical Assays

KLK6 Assays. KLK6 enzymatic activity was monitored in vitro by cleavage of the fluorogenic substrate N-Boc-FSR-AMC (Bachem) with a monochromator CLARIOstar® platereader (BMG LABTECH). In each well of a 384-well black plate, 5 µL of inhibitor (at different final assay concentrations, using either 1:2 or 1:3 dilutions) or DMSO control (final assay concentration 2%) were incubated with 5 µL KLK6 (final assay concentration 5 nM) in reaction buffer (50 mM Tris, 150 mM NaCl, 1 mM EDTA, 0.05% Tween-20, pH 7.5) for 30 min at rt. Then 10 µL of substrate (final assay concentration 20 µM) in reaction buffer were added to each well immediately before starting a kinetic measurement of fluorescence intensity (ex: 350-15, em: 440-20; every 60 s for 30 min). The slope of the measured signals was calculated using GraphPad Prism, normalized over the DMSO control (100% activity) and then used to generate dose-response curves. For k_{inact}/K_I determinations, a similar protocol was used with a final substrate concentration of 100 µM, which was added to inhibitor-enzyme solutions incubated for

different times for inhibitor and enzyme (usually 2, 5, 10, 20 and 40 min). For k_{off} determinations, 75 µL of inhibitor (at final assay saturating concentrations of 200 µM) or DMSO (final assay concentration 2%) were incubated with 75 µL of KLK6 (final assay concentration 50 nM) in reaction buffer for 1 h at rt. 130 µL of this mixture was then added to Zebaspin desalting columns (7K MWCO, 0.5 mL, Thermofisher) following standard desalting instructions. 10 µL aliquots from this mixture were tested at different time points by adding 10 µL of substrate (final assay concentration 20 µM) and residual activity was determined as mentioned above. Residual activity was plotted against time and the $t_{1/2}$ of the acyl enzyme complex was calculated with GraphPad Prism using the following curve fitting equation:

$$\boldsymbol{y = 100 * \left(1 - e^{-kx}\right)} \qquad \text{where} \quad \boldsymbol{t_{\frac{1}{2}} = \ln(2)\,/k}$$

Trypsin, Thrombin and Factor Xa Assays. The other serine proteases were obtained in high purity from commercial vendors and tested under the same assay conditions as KLK6. Final assay concentrations of the enzymes were: 3.5 ng/mL for trypsin; thrombin (> 2,800 NIH Units/mg protein) was diluted 1/10240; 16 nM for factor Xa.

KLK4 Assay. Pro-KLK4(200 µg/mL in activation buffer: 50 mM Tris, 10 mM $CaCl_2$, 150 mM NaCl, 0.05% Tween-20, pH 7.5), produced as describe above, was first activated via incubation with Thermolysin (Sigma Aldrich) (2 µg/mL) in a 1:1 mixture for 2 h at 37 °C. The reaction was stopped by adding an equal volume of EDTA (10 mM in assay buffer: 50 mM Tris, pH 9.0). The active KLK4 was further diluted in assay buffer (final assay concentration 1.25 µg/mL, corresponding to about 48 nM) and 5 µL of this solution were incubated with 5 µL of inhibitor (at different final assay concentrations, using either 1:2 or 1:3 dilutions) or DMSO control (final assay concentration 2%) for 30 min at rt. Then 10 µL of Boc-FSR-AMC (Bachem) (final assay concentration 15 µM) in assay buffer were used to initiate the reaction immediately before

starting a kinetic measurement of fluorescence intensity (ex: 350-15, em: 440-20; every 60 s for 20 min), using monochromator CLARIOstar® platereader (BMG LABTECH). The slope of the measured signals was calculated using GraphPad Prism, normalized over the DMSO control (100% activity) and used to generate dose-response curves.

Other KLK Assays. 50 µL of specified enzyme (final assay concentrations: 25 nM KLK5, 33 nM KLK7, 1.5 nM KLK8, 43 nM KLK13, 1 nM KLK14) in assay buffer (100mM phosphate buffer, 0.01% Tween-20, pH 8.5 for all KLKs) with each inhibitor concentration (1:3 dilutions) or DMSO control (2% final assay concentration) were incubated for 10 min at rt. Then 50 µL of specified substrate (Boc-ValProArg-AMC for all KLKs, except for KLK7: LeuLeuValTyr-AMC; 500 µM final assay concentration) were added to the mixture before starting a kinetic measurement of fluorescence intensity (ex: 380, em: 460; every 60 s for 30 min).

High-Throughput Screen

Optimization, miniaturization, pilot screen, the full HTS on a library of roughly 80,000 substances, and hit validation/selectivity screening against trypsin, thrombin, and Factor Xa was performed at the Chemical Biology Core Facility of the DKFZ/EMBL/University of Heidelberg using the biochemical assays described above.

Intact Protein Mass Spectrometry Analysis

Samples were prepared by mixing 2.5 µL inhibitor (final assay concentration 200 or 100 µM) or DMSO control (final assay concentration 2.7%) with 5 µL KLK6 (final assay concentration 7.3 µM) and aliquots from this mixture were analyzed at different time points (1 h, 3 h, 6 h, 24 h, and additionally 48 h and 72 h for selected compounds). Samples for full length measurements were acidified by adding TFA to a final concentration of 0.01% and injected directly on a self-packed analytical column (75 µm x 50 mm, POROS 10R1 (AB Applied Biosystems)) that served

as spray emitter as well. After loading the sample, an 8 min gradient from 3% to 95% acetonitrile at 300 nL/min was applied to elute bound proteins from the column. Eluting proteins were then analyzed by an online coupled Orbitrap Elite mass spectrometer (Thermo Fisher Scientific). Mass spectra were acquired at an *m/z* range of 400–3500 with a 240,000 resolution at 200 *m/z*. The gas pressure in the Orbitrap was manually reduced to stabilize protein ions during long transient times. Acquired data were deconvoluted using the Xtract deconvolution algorithm implemented in the XCalibur software (Thermo Fisher Scientific)**.**

Stability Assay.

Dulbeccos´s Modified Eagle´s Medium supplemented with 10% (v/v) fetal bovine serum, 2 mM L-glutamine and 1% penicillin/streptomycin was used to dilute the compounds 1:1000 (final assay concentration 10 µM, 0.2% DMSO). To each sample an internal standard containing a triazole as opposed to the ester bond was added (final assay concentration 10 µM), whose signal was used as internal reference to account for injection variability. The structure of the standard is the following:

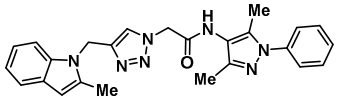

Internal standard for stability assays

Solutions were incubated at 37 °C and measured every hour until 10 h, followed by a final 24 h measurement. For the measurement, 10 µL of this solution were injected into an HPLC-MS system (Agilent 1260 Infinity and an ES quadrupole Agilent 6120; column: Kinetex® 2.6 µm C18 100 Å, LC Column 50 x 2.1 mm; Temperature = 40 ºC; Solvent A = water, 0.01% formic acid; Solvent B = acetonitrile, 0.01% formic acid; Flow Rate = 0.600 mL/min; method: Gradient: 99% A → 10% A [over 6 min] then 10% A → 1% A [over 2 min]) and "single ion mode" (SIM) was used to detect the target masses. Both entire compound and hydrolysis product

(corresponding alcohol) were detected with this system and quantified by integration of the area under the corresponding mass spectrum peak. Quantification (% of residual compound) was performed using the relative fraction of the compound measured peak area to the standard compound peak area. Relative fraction at t = 0 was used as 100%. GraphPad Prism was used to analyze the data, which were fitted to the following equation:

$$\boldsymbol{y = 100 * (e^{-kx})}$$

ABPs, Click Chemistry, and Pull-Down

Conditioned medium obtained from the different cell line cultures (v. infra) was concentrated using Vivaspin® filters (10 kDa cutoff) at 4000 rpm at 10 °C (volume usually reduced from 25 mL to 500 µL) and stored at –80 °C.

In-gel Fluorescence Procedure (Figure 7B): 1. To a sample of concentrated conditioned medium containing 20 µg of total protein (total protein concentration determined by DC protein assay (Bio Rad), using a BSA calibration curve) was added 60 ng of recombinant KLK6 or buffer. 2. Samples were incubated with **11**, **8**, or DMSO for 30 min at rt with shaking. 3. Compound **44** (final DMSO concentration 2%) was added and samples were incubated for 1 h at rt with shaking. 4. For every 100 µL of the protein sample was added 6 µL of a mixture containing 1 mM $CuSO_4$, 1 mM tris(2-carboxymethylphosphine) (TCEP), 100 µM tris(1-benzyl-1H-1,2,3-triazol-4-yl)methylamine (TBTA) and 100 µM of a TAMRA-labeled azide[40], and then incubated for 1 h at rt with shaking. 5. Reaction was stopped by the addition of two volumes of –20 °C acetone, and the samples were incubated at least 1 h at –80 °C, centrifuged (13,000 g) and the supernatant was discarded. 6 The obtained pellet was dissolved in 20% β-mercaptoethanol in Laemmli buffer, denatured for 5 min at 95 °C and half of the total sample was subjected to SDS-PAGE analysis.

Pull-down Procedure (Figures 7C and D): 1. Compound **44** at the specific concentration (final DMSO concentration 2%) was added to 200 μg of total protein and the sample was incubated for 1 h at rt with shaking. 2. The sample was handled as in steps 4 and 5 above, using a biotin-labeled azide instead of the TAMRA-lableled azide.[40] 3. The obtained pellet was dissolved in 200 μL of 2% SDS, 10 mM DTT in PBS (a 10 μL aliquot was removed for the BPD sample), and then incubated with agarose beads (Pierce™NeutrAvidin™Agarose, Thermofisher) for 2 h at rt with shaking. The supernatant was pipetted away from the beads and kept to make the SN sample. The beads were washed once with 1% SDS in PBS. 20 μL of 20% β-mercaptoethanol in Laemmli buffer was added to the sample and the beads were denatured for 10 min at 95 °C. The supernatant (the PD sample) was pipetted away from the beads. To the BPD and SN samples were added 5 μL of 20% β-mercaptoethanol in Laemmli buffer. The BPD, SN, and PD samples were then subjected to SDS-PAGE and WB.

SDS-PAGE and WB. 12% or 15% SDS-PAGE was freshly prepared prior to use. Running buffer for SDS-PAGE: 35 mM Tris, 285 mM glycine, 0.6% (w/v) SDS in Milli-Q® water. Gels were run for 15–20 min at 80 V, then for 120 min at 120 V. "In-gel" fluorescence was visualized with a Typhoon FLA 9500 Gel reader using Cy3/TAMRA setting (ex: 532 nm) at 600 PMT. When required, the SDS-gel was blotted on a methanol-activated nitrocellulose membrane for 60 min at 100 V (blotting buffer: 25 mM Tris, 192 mM glycine, 20% methanol) using a Bio-Rad Trans-Blot SD semi-dry transfer cell setup. The membrane was blocked in 5% milk powder with 1% Tween-20 PBS, washed once with 1% Tween-20 PBS, and incubated with KLK6 polyclonal antibody from rabbit (Abcam) overnight at 4 °C. The blot was washed 4 x 5 min with 1% Tween-20 PBS, incubated with secondary HRP-rabbit antibody (Advansta) for 1 h at rt, and

washed 4 x 5 min with 1% Tween-20 PBS prior to HRP substrate addition and chemiluminescence detection.

Cell culture

FaDu, Cal27, Detroit562, SCC9, VCap, U2OS and MiaPaca-2 were cultivated in Dulbeccos´s Modified Eagle´s Medium supplemented with 10% (v/v) fetal bovine serum, 2 mM L-glutamine and 1% penicillin/streptomycin. LNCap, and BxPC3 cells were cultivated in RPMI Medium supplemented with 10% (v/v) fetal bovine serum. All cell lines were grown at 37 °C under a humidified atmosphere supplied with 5% CO_2. Culture medium was exchanged to non-supplemented RPMI (phenol red free) 48 h prior to collection and concentration of conditioned medium for ABPs experiments.

Cell-based Assay: 20,000 cells were seeded on sterile coverslips in a 12-well plate and cultured with indicated concentrations of **8** or **11**, respectively, or DMSO as control with daily medium exchange for 48–72 hours. BrdU labeling and detection as well as phalloidin and nuclear staining with Hoechst 33342 were done as described elsewhere.[17,41] Coverslips were mounted with VectaMount (Vector Laboratories) and were analyzed by fluorescence microscopy (Olympus BX-50F). Pictures were taken from at least five individual areas using the Olympus XC30 camera and proliferation was assessed by the amount of BrdU-positive cells divided by the total amount of cells. Authentication of all cell lines used in this assay was confirmed by the Multiplex Human Cell Line Authentication Test (Multiplexion, Germany).

Docking studies

11 was docked into a crystal structure of KLK6 bound with inhibitor **6** (PDB: 4D8N). Structure preparation and docking experiments were carried out in the Schrödinger Suite.[42] The force field applied in the modeling process was OPLS_2005. The Protein Preparation Wizard

was used to detect and fix problems in the protein structure, assign the protonation state of acidic and basic residues at pH 7.0 ± 2.0, optimize the H-bond network, and finally carry out a restrained minimization to refine the geometry. Crystal water molecules were removed in order not to interfere with the docking process. The receptor grid was calculated with the default force field parameters, i.e. a Van der Waals radius scaling factor of 1.0 and a partial charge cutoff of 0.25 Å. The binding site was defined as a box centered on the centroid of the co-crystallized ligand and its side length was set to 20 Å. No constraints were applied. **11** was prepared with LigPrep. Possible protonation states at pH 7.0 ± 2.0 were enumerated by Epik, tautomerized and low-energy 3D structures were produced. The flexible ligand docking was performed in Glide using the XP Extra Precision. The default force field parameters were assigned to the atoms of **11**, consisting in scaling down the Van der Waals radii by 0.8 and setting the partial charge cutoff to 0.15 Å. The poses were subjected to a post-docking minimization and selected according to their docking score and by visual inspection. The CovDock protocol of Schrödinger was applied to generate the tetrahedral intermediate formed by the nucleophilic addition of the hydroxyl oxygen atom of Ser195 on the acyl carbon atom of **11**: 1. The reactive residue was first mutated to alanine to eliminate any bias induced by the sidechain conformation; 2. Non-covalent docking was performed by Glide with positional constraints between the attachment atoms of **11** and KLK6; 3. The reactive residue was restored and geometrical criteria were used to select the poses that could form covalent linkages; 4. Prime was applied to optimize the ligand and the reactive residue; 5. The affinity of a given pose was estimated from both the Glide score of the noncovalent binding prior to reaction and the Glide score of the covalent final binding mode. In order to prepare the docking procedure, the center of the box enclosing the binding site was defined as the centroid of a pose of **11** previously generated by noncovalent docking. The

"nucleophilic addition on a double bond" option was selected as the reaction type. As **11** contains an ester and an amide functions, the relevant SMARTS pattern was defined to target the correct carbonyl group during the reaction. All the parameters related to the refinement step were kept to their default values.

ASSOCIATED CONTENT

Supporting Information

The Supporting Information is available free of charge on the ACS Publications website at DOI: XXXX.

Supplementary figures, primers, tryptic digest mass spectrometry analysis, compound synthesis, characterization data and ^{1}H and ^{13}C spectra (PDF).

Molecular formula strings, biochemical data against KLK6 and trypsin (CSV).

Model of **11** docked into 4D8N overlaid with 1L2E (PDB).

AUTHOR INFORMATION

Corresponding Author

* aubry.miller@dkfz.de

Present Addresses

† Genomics and Proteomics Core Facility, German Cancer Research Center (DKFZ), Heidelberg, Germany

ORCID

Elena De Vita: 0000-0003-4707-8342

Edward W. Tate: 0000-0003-2213-5814

Aubry K. Miller: 0000-0002-1761-4143

Author Contributions

Research design by E.D.V., P.S., N.G., and A.K.M; Chemical synthesis by E.D.V., P.S., J.L., S.K., and A.K.M.; Mass experiments by E.D.V. and B.H.; Molecular docking by V.H.; Protein production by E.D.V., E.R., A.S., and N.P.; Biochemical assays by E.D.V.; ABPs development by E.D.V., S.L., and E.W.T.; Cellular assay by J.H.; Data analysis and manuscript preparation by E.D.V. and A.K.M.. All authors have given approval to the final version of the manuscript.

Notes

The authors declare no competing financial interests.

ACKNOWLEDGMENT

This work was supported in part by the Cooperation Program in Cancer Research of the Deutsches Krebsforschungszentrum (DKFZ) and Israel's Ministry of Science, Technology and Space (MOST) (GR-2495 to N.P. and A.K.M), and by the German Cancer Aid (70112000, to J.H.). E.D.V. was supported by an EMBO short-term fellowship (STF7471). Further financial support from the Helmholtz Drug Initiative and the German Cancer Consortium (DKTK) is gratefully acknowledged. We thank Eugene Gbekor, Dr. Ulrike Uhrig, and Dr. Joe Lewis of the DKFZ Chemical Biology Core Facility for support in performing and analyzing the data from the HTS. We thank Dr. Kim Remans and Ines Racke of the EMBL Protein Production Facility for

support in producing KLK6. We thank Vani Verma for technical chemical assistance, Kathrin Jacob for performing the cell-based assay, Antje Schuhmann and Nataly Henfling for technical assistance with cell culture models, and Dr. Karel Klika and Gabriele Schwebel for NMR spectroscopy support. We thank Sabine Fiedler and Martina Schnölzer at the DKFZ Genomics and Proteomics Core Facility for performing the tryptic digestion and relative analyses. We thank Dr. Matthias Mayer (ZMBH) for helpful suggestions in the development of the k_{off} assay. Protein X-ray graphics and analyses were performed with the UCSF Chimera package. Chimera is developed by the Resource for Biocomputing, Visualization, and Informatics at the University of California, San Francisco (supported by NIGMS P41-GM103311).

ABBREVIATIONS

KLKs, tissue kallikreins; KLK6, kallikrein-related peptidase 6; ABP, activity-based probe; PSA, prostate-specific antigen; EMT; epithelial to mesenchymal transition; PAR, protease-activated receptor; AEBSF, 4-(2-aminoethyl)benzenesulfonyl fluoride; C.I., confidence interval; DMEM, Dulbecco's modified Eagle's medium; BrdU, 5-bromo-2'-deoxyuridine; shRNA, short hairpin RNA; CuAAC, Copper-catalyzed alkyne–azide cycloaddition; CuTC, copper-2-thiophenecarboxylate; TFP, tri-2-furylphosphine; EDCI, N-(3-Dimethylaminopropyl)-N′-ethylcarbodiimide hydrochloride; HATU, 1-[Bis(dimethylamino)methylene]-1H-1,2,3-triazolo[4,5-b]pyridinium 3-oxide hexafluorophosphate.

REFERENCES

(1) (a) Prassas, I.; Eissa, A.; Poda, G.; Diamandis, E. P. Unleashing the therapeutic potential of human kallikrein-related serine proteases. *Nat. Rev. Drug Discovery* **2015**, *14,* 183–202; (b) Brattsand, M.; Stefansson, K.; Lundh, C.; Haasum, Y.; Egelrud, T. A proteolytic cascade of

kallikreins in the stratum corneum. *J. Invest. Dermatol.* **2005**, *124,* 198 –203; (c) Sotiropoulou, G.; Pampalakis, G. Kallikrein-related peptidases: Bridges between immune functions and extracellular matrix degradation. *Biol. Chem.* **2010**, *391,* 321–331.

(2) Shaw, J. L. V.; Diamandis, E. P. Distribution of 15 human kallikreins in tissues and biological fluids. *Clin. Chem. (Washington, DC, U. S.)* **2007**, *53,* 1423–1432.

(3) (a) Filippou, P. S.; Karagiannis, G. S.; Musrap, N.; Diamandis, E. P. Kallikrein-related peptidases (KLKs) and the hallmarks of cancer. *Crit. Rev. Clin. Lab. Sci.* **2016**, *53,* 277–291; (b) Kryza, T.; Silva, M. L.; Loessner, D.; Heuze-Vourc'h, N.; Clements, J. A. The kallikrein-related peptidase family: dysregulation and functions during cancer progression. *Biochimie* **2016**, *122,* 283–299.

(4) Kontos, C. K.; Scorilas, A. Kallikrein-related peptidases (KLKs): a gene family of novel cancer biomarkers. *Clin. Chem. Lab. Med.* **2012**, *58,* 1877–1891.

(5) (a) LeBeau, A. M.; Kostova, M.; Craik, C. S.; and Denmeade, S. R. Prostate-specific antigen: an overlooked candidate for the targeted treatment and selective imaging of prostate cancer. *J. Biol. Chem.* **2010**, *391,* 333–343; (b) Koistinen, H.; Mattsson, J.; Stenman, U.-h. KLK-targeted therapies for prostate cancer. *eJIFCC* **2014**, *25,* 207–218.

(6) Oikonomopoulou, K.; Hansen, K. K.; Baruch, A.; Hollenberg, M. D.; Diamandis, E. P. Immunofluorometric activity-based probe analysis of active KLK6 in biological fluids. *Biol. Chem.* **2008**, *389,* 747–756.

(7) (a) Anisowicz, A.; Sotiropoulou, G.; Stenman, G.; Mok, S. C.; Sager, R. A novel protease homolog differentially expressed in breast and ovarian cancer. *Mol. Med. (Cambridge, MA, U.*

S.) **1996**, *2,* 624–636; (b) Scarisbrick, I. a.; Towner, M. D.; Isackson, P. J. Nervous system-specific expression of a novel serine protease: regulation in the adult rat spinal cord by excitotoxic injury. *J. Neurosci.* **1997**, *17,* 8156–8168; (c) Yamashiro, K.; Tsuruoka, N.; Kodama, S.; Tsujimoto, M.; Yamamura, Y.; Tanaka, T.; Nakazato, H.; Yamaguchi, N. Molecular cloning of a novel trypsin-like serine protease (neurosin) preferentially expressed in brain. *Biochim. Biophys. Acta, Gene Struct. Expression* **1997**, *1350,* 11–14; (d) Little, S. P.; Dixon, E. P.; Norris, F.; Buckley, W.; Becker, G. W.; Johnson, M.; Dobbins, J. R.; Wyrick, T.; Miller, J. R.; MacKellar, W.; Hepburn, D.; Corvalan, J.; McClure, D.; Liu, X.; Stephenson, D.; Clemens, J.; Johnstone, E. M. Zyme, a novel and potentially amyloidogenic enzyme cDNA isolated from Alzheimer's disease brain. *J. Biol. Chem.* **1997**, *272,* 25135–25142.

(8) Blaber, S. I.; Yoon, H.; Scarisbrick, I. A.; Juliano, M. A.; Blaber, M. The autolytic regulation of human kallikrein-related peptidase 6. *Biochemistry* **2007**, *46,* 5209–5217.

(9) (a) Bayani, J.; Diamandis, E. P. The physiology and pathobiology of human kallikrein-related peptidase 6 (KLK6). *Clin. Chem. Lab. Med.* **2012**, *50,* 211–233; (b) Pampalakis, G.; Sykioti, V.-S.; Ximerakis, M.; Stefanakou-Kalakou, I.; Melki, R.; Vekrellis, K.; Sotiropoulou, G. KLK6 proteolysis is implicated in the turnover and uptake of extracellular alpha-synuclein species. *Oncotarget* **2017**, *8,* 14502–14515.

(10) (a) Yoon, H.; Radulovic, M.; Scarisbrick, I. A. Kallikrein-related peptidase 6 orchestrates astrocyte form and function through proteinase activated receptor-dependent mechanisms. *Biol. Chem.* **2018**, *399*, 1041–1052; (b) Hollenberg, M. D. KLKs and their hormone-like signaling actions: a new life for the PSA-KLK family. *Biol. Chem.* **2014**, *395,* 915–929; (c) Oikonomopoulou, K.; Hansen, K. K.; Saifeddine, M.; Tea, I.; Blaber, M.; Blaber, S. I.;

Scarisbrick, I.; Andrade-Gordon, P.; Cottrell, G. S.; Bunnett, N. W.; Diamandis, E. P.; Hollenberg, M. D. Proteinase-activated receptors, targets for kallikrein signaling. *J. Biol. Chem.* **2006**, *281,* 32095–32112; (d) Caliendo, G.; Santagada, V.; Perissutti, E.; Severino, B.; Fiorino, F.; Frecentese, F.; Juliano, L. Kallikrein protease activated receptor (PAR) axis: an attractive target for drug development. *J. Med. Chem.* **2012**, *55*, 6669–6686.

(11) Patra, K.; Soosaipillai, A.; Sando, S. B.; Lauridsen, C.; Berge, G.; Moller, I.; Grontvedt, G. R.; Brathen, G.; Begcevic, I.; Moussaud, S.; Minthon, L.; Hansson, O.; Diamandis, E. P.; White, L. R.; Nielsen, H. M. Assessment of kallikrein 6 as a cross-sectional and longitudinal biomarker for Alzheimer's disease. *Alzheimer's Res. Ther.* **2018**, *10,* 1–11.

(12) (a) Blaber, S. I.; Ciric, B.; Christophi, G. P.; Bernett, M. J.; Blaber, M.; Rodriguez, M.; Scarisbrick, I. A. Targeting kallikrein 6 proteolysis attenuates CNS inflammatory disease. *FASEB J* **2004**, *18,* 920–922; (b) Scarisbrick, I. A.; Yoon, H.; Panos, M.; Larson, N.; Blaber, S. I.; Blaber, M.; Rodriguez, M. Kallikrein 6 regulates early CNS demyelination in a viral model of multiple sclerosis. *Brain Pathol.* **2012**, *22,* 709–722.

(13) Krenzer, S.; Peterziel, H.; Mauch, C.; Blaber, S. I.; Blaber, M.; Angel, P.; Hess, J. Expression and function of the kallikrein-related peptidase 6 in the human melanoma microenvironment. *J. Invest. Dermatol.* **2011**, *131,* 2281–2288.

(14) Prezas, P.; Arlt, M. J. E.; Viktorov, P.; Soosaipillai, A.; Holzscheiter, L.; Schmitt, M.; Talieri, M.; Diamandis, E. P.; Krüger, A.; Magdolen, V. Overexpression of the human tissue kallikrein genes KLK4, 5, 6, and 7 increases the malignant phenotype of ovarian cancer cells. *Biol. Chem.* **2006**, *387,* 807–811.

(15) Kim, T. W.; Lee, S.-J.; Kim, J.-T.; Kim, S. J.; Min, J.-K.; Bae, K.-H.; Jung, H.; Kim, B.-Y.; Lim, J.-S.; Yang, Y.; Yoon, D.-Y.; Choe, Y.-K.; Lee, H. G. Kallikrein-related peptidase 6 induces chemotherapeutic resistance by attenuating auranofin-induced cell death through activation of autophagy in gastric cancer. *Oncotarget* **2016**, *7,* 85332–85348.

(16) Drucker, K. L.; Paulsen, A. R.; Giannini, C.; Decker, P. A.; Blaber, S. I.; Blaber, M.; Uhm, J. H.; O'Neill, B. P.; Jenkins, R. B.; Scarisbrick, I. A. Clinical significance and novel mechanism of action of kallikrein 6 in glioblastoma. *Neuro-Oncology (Cary, NC, U. S.)* **2013**, *15,* 305–318.

(17) Schrader, C. H.; Kolb, M.; Zaoui, K.; Flechtenmacher, C.; Grabe, N.; Weber, K. J.; Hielscher, T.; Plinkert, P. K.; Hess, J. Kallikrein-related peptidase 6 regulates epithelial-to-mesenchymal transition and serves as prognostic biomarker for head and neck squamous cell carcinoma patients. *Mol. Cancer* **2015**, *14,* 1–14.

(18) (a) Goettig, P.; Magdolen, V.; Brandstetter, H. Natural and synthetic inhibitors of kallikrein-related peptidases (KLKs). *Biochimie* **2010**, *92,* 1546–1567; (b) Swedberg, J. E.; De Veer, S. J.; Harris, J. M. Natural and engineered kallikrein inhibitors: an emerging pharmacopoeia. *Biol. Chem.* **2010**, *391,* 357–374; (c) Sotiropoulou, G.; Pampalakis, G. Targeting the kallikrein-related peptidases for drug development. *Trends Pharmacol. Sci.* **2012**, *33,* 623–634; (d) Masurier, N.; Arama, D. P.; El Amri, C.; Lisowski, V. Inhibitors of kallikrein-related peptidases: an overview. *Med. Res. Rev.* **2018**, *38,* 655–683.

(19) (a) Cohen, I.; Naftaly, S.; Ben-Zeev, E.; Hockla, A.; Radisky, E. S.; Papo, N. Pre-equilibrium competitive library screening for tuning inhibitor association rate and specificity toward serine proteases. *Biochem. J.* **2018**, *475,* 1335–1352; (b) Sananes, A.; Cohen, I.; Shahar,

A.; Hockla, A.; De Vita, E.; Miller, A. K.; Radisky, E. S.; and Papo, N. A potent, proteolysis-resistant inhibitor of kallikrein-related peptidase 6 (KLK6) for cancer therapy, developed by combinatorial engineering. *J. Biol. Chem.* **2018**, *293*, 12663–12680; (c) Chen, W.; Kinsler, V. A.; Macmillan, D.; Di, W.-L. Tissue kallikrein inhibitors based on the sunflower trypsin inhibitor scaffold – a potential therapeutic intervention for skin diseases. *PLoS One* **2016**, *11,* e0166268.

(20) (a) de Veer, S. J.; Furio, L.; Swedberg, J. E.; Munro, C. A.; Brattsand, M.; Clements, J. A.; Hovnanian, A.; Harris, J. M. Selective substrates and inhibitors for kallikrein-related peptidase 7 (KLK7) shed light on KLK proteolytic activity in the stratum corneum. *J. Invest. Dermatol.* **2017**, *137,* 430–439; (b) Linschoten, M. New Kallikrein 7 Inhibitors. WO 2015/112079 A1, 2015.

(21) (a) Liang, G.; Chen, X.; Aldous, S.; Pu, S. F.; Mehdi, S.; Powers, E.; Xia, T.; Wang, R. Human kallikrein 6 inhibitors with a para-amidobenzylanmine P1 group identified through virtual screening. *Bioorg. Med. Chem. Lett.* **2012**, *22,* 2450–2455; (b) Liang, G.; Chen, X.; Aldous, S.; Pu, S. F.; Mehdi, S.; Powers, E.; Giovanni, A.; Kongsamut, S.; Xia, T.; Zhang, Y.; Wang, R.; Gao, Z.; Merriman, G.; McLean, L. R.; Morize, I. Virtual screening and x-ray crystallography for human kallikrein 6 inhibitors with an amidinothiophene p1 group. *ACS Med. Chem. Lett.* **2012**, *3,* 159–164.

(22) Severino, B.; Fiorino, F.; Corvino, A.; Caliendo, G.; Santagada, V.; Assis, D. M.; Oliveira, J. R.; Juliano, L.; Manganelli, S.; Benfenati, E.; Frecentese, F.; Perissutti, E.; Juliano, M. A. Synthesis, biological evaluation, and docking studies of PAR2-AP-derived pseudopeptides as inhibitors of kallikrein 5 and 6. *Biol. Chem.* **2015**, *396,* 45–52.

(23) Soualmia, F.; Bosc, E.; Amiri, S. A.; Stratmann, D.; Magdolen, V.; Darmoul, D.; Reboud-Ravaux, M.; Amri, C. E. Insights into the activity control of the kallikrein-related peptidase 6: small-molecule modulators and allosterism. *Biol. Chem.* **2017**, *399*, 1073–1078.

(24) (a) Miura, M.; Seki, N.; Koike, T.; Ishihara, T.; Niimi, T.; Hirayama, F.; Shigenaga, T.; Sakai-Moritani, Y.; Kawasaki, T.; Sakamoto, S.; Okada, M.; Ohta, M.; Tsukamoto, S. i. Potent and selective TF/FVIIa inhibitors containing a neutral P1 ligand. *Bioorg. Med. Chem.* **2006**, *14,* 7688–7705; (b) Bolton, S. A.; Sutton, J. C.; Anumula, R.; Bisacchi, G. S.; Jacobson, B.; Slusarchyk, W. A.; Treuner, U. D.; Wu, S. C.; Zhao, G.; Pi, Z.; Sheriff, S.; Smirk, R. A.; Bisaha, S.; Cheney, D. L.; Wei, A.; Schumacher, W. A.; Hartl, K. S.; Liu, E.; Zahler, R.; Seiler, S. M. Discovery of nonbenzamidine factor VIIa inhibitors using a biaryl acid scaffold. *Bioorg. Med. Chem. Lett.* **2013**, *23,* 5239–5243; (c) Wurtz, N. R.; Parkhurst, B. L.; Jiang, W.; DeLucca, I.; Zhang, X.; Ladziata, V.; Cheney, D. L.; Bozarth, J. R.; Rendina, A. R.; Wei, A.; Luettgen, J. M.; Wu, Y.; Wong, P. C.; Seiffert, D. A.; Wexler, R. R.; Priestley, E. S. Discovery of phenylglycine lactams as potent neutral factor VIIa inhibitors. *ACS Med. Chem. Lett.* **2016**, *7,* 1077–1081; (d) Cheney, D. L.; Bozarth, J. M.; Metzler, W. J.; Morin, P. E.; Mueller, L.; Newitt, J. A.; Nirschl, A. H.; Rendina, A. R.; Tamura, J. K.; Wei, A.; Wen, X.; Wurtz, N. R.; Seiffert, D. A.; Wexler, R. R.; Priestley, E. S. Discovery of novel P1 groups for coagulation factor VIIa inhibition using fragment-based screening. *J. Med. Chem.* **2015**, *58,* 2799–2808; (e) Venkatraj, M., Messagie, J., Joossens, J., Lambeir, A. M., Haemers, A., Van Der Veken, P., and Augustyns, K. Synthesis and evaluation of non-basic inhibitors of urokinase-type plasminogen activator (uPA). *Bioorg. Med. Chem.* **2012**, *20*, 1557–1568.

(25) (a) Fevig, J. M.; Pinto, D. J.; Han, Q.; Quan, M. L.; Pruitt, J. R.; Jacobson, I. C.; Galemmo, J. R. A., Robert A.; Wang, S.; Orwat, M. J.; Bostrom, L. L.; Knabb, R. M.; Wong, P.

C.; Lam, P. Y. S.; Wexler, R. R. Synthesis and SAR of benzamidine factor Xa inhibitors containing a vicinally-substituted heterocyclic core. *Bioorg. Med. Chem. Lett.* **2001**, *11,* 641–645; (b) Rai, R.; Kolesnikov, A.; Sprengeler, P. A.; Torkelson, S.; Ton, T.; Katz, B. A.; Yu, C.; Hendrix, J.; Shrader, W. D.; Stephens, R.; Cabuslay, R.; Sanford, E.; Young, W. B. Discovery of novel heterocyclic factor VIIa inhibitors. *Bioorg. Med. Chem. Lett.* **2006**, *16,* 2270–2273.

(26) (a) Liang, G.; Bowen, J. P. Development of trypsin-like serine protease inhibitors as therapeutic agents: opportunities, challenges, and their unique structure-based rationales. *Curr. Top. Med. Chem. (Hilversum, Neth.)* **2016**, *16,* 1506–1529; (b) Liang, G.; Choi-Sledeski, Y. M.; Chen, X.; Gong, Y.; MacMillan, E. W.; Tsay, J.; Sides, K.; Cairns, J.; Kulitzscher, B.; Aldous, D. J.; Morize, I.; Pauls, H. W. Dimerization of beta-tryptase inhibitors, does it work for both basic and neutral P1 groups? *Bioorg Med Chem Lett* **2012**, *22,* 3370–3376.

(27) Hereafter, KLK6 refers to this triple mutant.

(28) Hackl, M. W.; Lakemeyer, M.; Dahmen, M.; Glaser, M.; Pahl, A.; Lorenz-Baath, K.; Menzel, T.; Sievers, S.; Böttcher, T.; Antes, I.; Waldmann, H.; Sieber, S. A. Phenyl esters are potent inhibitors of caseinolytic protease P and reveal a stereogenic switch for deoligomerization. *J. Am. Chem. Soc.* **2015**, *137,* 8475–8483.

(29) Carbamates are known to react with serine proteases. See: Alexander, J. P.; Cravatt, B. F. Mechanism of carbamate inactivation of FAAH: implications for the design of covalent inhibitors and in vivo functional probes for enzymes. *Chem. Biol.* **2005**, *12,* 1179–1187.

(30) Copeland, R. A., *Evaluation of Enzyme Inhibitors in Drug Discovery. A Guide for Medicinal Chemists and Pharmacologists*. John Wiley & Sons, Inc.: Hoboken, New Jersey, 2013.

(31) Maibaum, J.; Liao, S. M.; Vulpetti, A.; Ostermann, N.; Randl, S.; Rüdisser, S.; Lorthiois, E.; Erbel, P.; Kinzel, B.; Kolb, F. A.; Barbieri, S.; Wagner, J.; Durand, C.; Fettis, K.; Dussauge, S.; Hughes, N.; Delgado, O.; Hommel, U.; Gould, T.; Sweeney, A. M.; Gerhartz, B.; Cumin, F.; Flohr, S.; Schubart, A.; Jaffee, B.; Harrison, R.; Risitano, A. M.; Eder, J.; Anderson, K. Small-molecule factor D inhibitors targeting the alternative complement pathway. *Nat. Chem. Biol.* **2016**, *12,* 1105–1110.

(32) (a) Oikonomopoulou, K.; Batruch, I.; Smith, C. R.; Soosaipillai, A.; Diamandis, E. P.; Hollenberg, M. D. Functional proteomics of kallikrein-related peptidases in ovarian cancer ascites fluid. *Biol. Chem.* **2010**, *391,* 381–390; (b) Dorn, J.; Beaufort, N.; Schmitt, M.; Diamandis, E. P.; Goettig, P.; Magdolen, V. Function and clinical relevance of kallikrein-related peptidases and other serine proteases in gynecological cancers. *Crit. Rev. Clin. Lab. Sci.* **2014**, *51,* 63–84.

(33) Paulick, M. G.; Bogyo, M. Application of activity-based probes to the study of enzymes involved in cancer progression. *Curr. Opin. Genet. Dev.* **2008**, *18,* 97–106.

(34) (a) Deu, E.; Verdoes, M.; Bogyo, M. New approaches for dissecting protease functions to improve probe development and drug discovery. *Nat. Struct. Mol. Biol.* **2012**, *19,* 9–16; (b) Fonović, M.; Bogyo, M. Activity based probes for proteases: applications to biomarker discovery, molecular imaging and drug screening. *Curr. Pharm. Des.* **2007**, *13,* 253–261; (c) Wright, M. H.; Sieber, S. A. Chemical proteomics approaches for identifying the cellular targets of natural products. *Nat. Prod. Rep.* **2016**, *33,* 681–708; (d) Heal, W. P.; Dang, T. H.; Tate, E. W. Activity-based probes: discovering new biology and new drug targets. *Chem. Soc. Rev* **2011**, *40,* 246–257; (e) Kasperkiewicz, P.; Poreba, M.; Groborz, K.; Drag, M. Emerging challenges in

the design of selective substrates, inhibitors and activity-based probes for indistinguishable proteases. *The FEBS journal* **2017**, *284,* 1518–1539.

(35) Lawrence, M. G.; Lai, J.; Clements, J. A. Kallikreins on steroids: structure, function, and hormonal regulation of prostate-specific antigen and the extended kallikrein locus. *Endocr. Rev.* **2010**, *31,* 407–446.

(36) Kuzmanov, U.; Jiang, N.; Smith, C. R.; Soosaipillai, A.; Diamandis, E. P. Differential *N*-glycosylation of kallikrein 6 derived from ovarian cancer cells or the central nervous system. *Mol. Cell. Proteomics* **2009**, *8,* 791–798.

(37) Kusturin, C. L.; Liebeskind, L. S.; Neumann, W. L. A new catalytic cross-coupling approach for the synthesis of protected aryl and heteroaryl amidines. *Org. Lett.* **2002**, *4,* 983–985.

(38) Bernett, M. J.; Blaber, S. I.; Scarisbrick, I. A.; Dhanarajan, P.; Thompson, S. M.; Blaber, M., Crystal structure and biochemical characterization of human kallikrein 6 reveals that a trypsin-like kallikrein is expressed in the central nervous system. *J. Biol. Chem.* **2002,** *277*, 24562–24570.

(39) (a) Borgono, C. A.; Michael, I. P.; Shaw, J. L.; Luo, L. Y.; Ghosh, M. C.; Soosaipillai, A.; Grass, L.; Katsaros, D.; Diamandis, E. P., Expression and functional characterization of the cancer-related serine protease, human tissue kallikrein 14. *J. Biol. Chem.* **2007,** *282*, 2405–2422; (b) Michael, I. P.; Sotiropoulou, G.; Pampalakis, G.; Magklara, A.; Ghosh, M.; Wasney, G.; Diamandis, E. P., Biochemical and enzymatic characterization of human kallikrein 5 (hK5), a novel serine protease potentially involved in cancer progression. *J. Biol. Chem.* **2005,** *280*, 14628–14635; (c) Yu, Y.; Prassas, I.; Dimitromanolakis, A.; Diamandis, E. P. Novel biological

substrates of human kallikrein 7 identified through degradomics. *J. Biol. Chem.* **2005**, *290*, 17762–17775. (d) Eissa, A.; Amodeo, V.; Smith, C. R.; Diamandis, E. P., Kallikrein-related peptidase-8 (KLK8) is an active serine protease in human epidermis and sweat and is involved in a skin barrier proteolytic cascade. *J. Biol. Chem.* **2011,** *286*, 687–706; (e) Sotiropoulou, G.; Rogakos, V.; Tsetsenis, T.; Pampalakis, G.; Zafiropoulos, N.; Simillides, G.; Yiotakis, A.; Diamandis, E. P., Emerging interest in the kallikrein gene family for understanding and diagnosing cancer. *Oncol. Res.* **2002,** *13*, 381–391.

(40) TAMRA-labeled and biotin-labeled azides are respectively compounds **2** and **3** from: Broncel, M; Serwa, R. A.; Ciepla, P.; Krause, E.; Dallman, M.J.; Magee, A. I.; Tate, E. W. Multifunctional reagents for quantitative proteome-wide analysis of protein modification in human cells and dynamic profiling of protein lipidation during vertebrate development. *Angew. Chem. Int. Ed.* **2015**, *54,* 5948–5951.

(41) Klucky, B.; Mueller, R.; Vogt, I.; Teurich, S.; Hartenstein, B.; Breuhahn, K.; Flechtenmacher, C.; Angel, P.; Hess, J. Kallikrein 6 induces E-cadherin shedding and promotes cell proliferation, migration, and invasion. *Cancer Res.* **2007**, *67,* 8198–8206.

(42) Schrödinger Suite. Schrödinger, LLC; New York, NY: 2015.

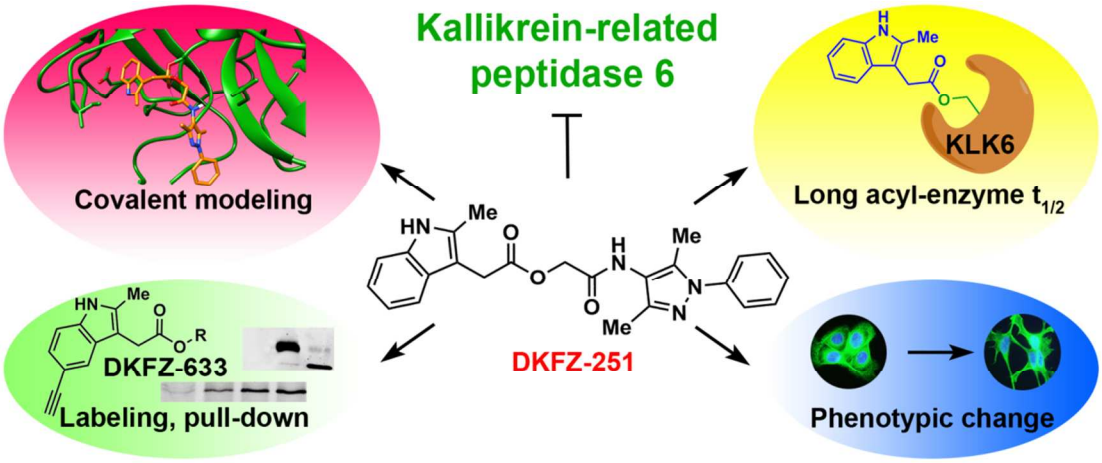
Kallikrein-related peptidase 6
Covalent modeling
KLK6
Long acyl-enzyme $t_{1/2}$
DKFZ-633
Labeling, pull-down
DKFZ-251
Phenotypic change